Vol. 680: 111–136, 2021
https://doi.org/10.3354/meps13853

MARINE ECOLOGY PROGRESS SERIES
Mar Ecol Prog Ser

Published December 9

Contribution to the Theme Section 'Advancing dynamic modelling of marine populations and ecosystems'

Climate variation and anchovy recruitment in the California Current: a cause-and-effect analysis of an end-to-end model simulation

D. V. Politikos[1,6,*], K. A. Rose[2], E. N. Curchitser[1], D. M. Checkley Jr.[3], R. R. Rykaczewski[4], J. Fiechter[5]

[1]Department of Environmental Sciences, Rutgers University, New Brunswick, NJ 08901, USA
[2]University of Maryland Center for Environmental Science, Horn Point Laboratory, Cambridge, MD 21613, USA
[3]Scripps Institution of Oceanography, University of California, San Diego, La Jolla, CA 92093, USA
[4]Ecosystem Sciences Division, NOAA Pacific Islands Fisheries Science Center, Honolulu, HI, 96818-5007, USA
[5]Ocean Sciences Department, University of California, Santa Cruz, CA 95064, USA
[6]*Present address:* Institute of Marine Biological Resources and Inland Waters, Hellenic Centre for Marine Research, 16452, Attica, Greece

ABSTRACT: Interannual and regime (decadal) scale changes in climate affect the spatial distribution and productivity of marine fish species in numerous ecosystems. We analyzed a historical simulation (1965–2000) from an end-to-end ecosystem model of anchovy population dynamics for the California Current System to untangle the effects of warm versus cool conditions on recruitment. A 3-dimensional coupled hydrodynamic-NPZD (nitrogen-phytoplankton-zooplankton-detritus) model (ROMS-NEMURO) provided the physical conditions (circulation, temperature) and 3 zooplankton concentrations as inputs to an anchovy full life cycle individual-based model (IBM). Our analysis was focused on isolating the effects of the well-documented El Niño Southern Oscillation signal and 3 climate regimes on spawning habitat, development, and survival of eggs and yolk-sac larvae, growth and survival of larvae and juveniles, and ultimately recruitment of anchovy. The major drivers of lowered recruitment success in warm years and in warmer regimes were reduced survival and growth rates of eggs and larvae that resulted from the poleward shift of adults in response to warmer temperatures prior to spawning. Three model-data comparisons showed the model deviated from empirically derived values of annual recruitment success but agreed with data for annual mean latitude of egg distributions and predicted larval consumption rates versus measured zooplankton concentrations. More effort is needed to improve certain biological aspects of the IBM so that it can replicate empirically estimated recruitment fluctuations. Overall, the altered responses of anchovy to changing climate in the California Current domain illustrate the benefit of the present mechanistic approach to infer how anchovy may respond under future ecosystem conditions.

KEY WORDS: Northern anchovy · Climate variation · California Current · Recruitment · End-to-end model · Regime shift

1. INTRODUCTION

Climate regime shifts and the El Niño Southern Oscillation (ENSO) are conspicuous climate phenomena that cause drastic changes in the functioning of marine ecosystems (Doney et al. 2012). Fish populations have been affected by these phenomena in various ways, such as geographic shifts in their distribution and phenology (Drinkwater 2005, Perry et al. 2005, Rose 2005, Sundby & Nakken 2008, Overholtz et al. 2011, Shoji et al. 2011, Jung et al. 2014, Asch 2015, Walsh et al. 2015) and signif-

*Corresponding author: dimpolitik@gmail.com

icant changes in their growth, survival, and recruitment (Fiedler et al. 1986, Clark et al. 1999, Brunel & Boucher 2007, Takahashi et al. 2009). Understanding the underlying relationships between past environmental variability and fish population dynamics is needed to reliably project how these populations will respond to ongoing climate change (King et al. 2015). Establishing links between environmental and population variability can also inform management and policy decisions (Hofmann & Powell 1998, King et al. 2015).

Northern anchovy is an ecologically important small pelagic fish species in the California Current System (CCS) that inhabits coastal upwelling areas and showed decadal population cycles with sardine during the last century (Checkley et al. 2009, 2017, McClatchie 2014). The long-standing idea of high asynchrony between anchovy and sardine populations across ecosystems around the world has recently been questioned, because the 2 species do not show similar peak biomasses (i.e. are not replacing each other in the ecosystem), and the statistical evidence for the population asynchrony relied on relatively short time series of landings data (Siple et al. 2020). The population dynamics of both species remain a topic of discussion and analyses (Nakayama et al. 2018, Salvatteci et al. 2018, Canales et al. 2020, Sydeman et al. 2020).

Northern anchovy consumes larger planktonic organisms (e.g. diatoms, copepods) and remains closer to the coast than sardines. Anchovy releases multiple egg batches within an extended spawning period that lasts from late winter to spring (Checkley et al. 2009, Rose et al. 2015). Over the last century, the physical and biological conditions in the CCS have been influenced by multidecadal climate regime shifts related to the interannual ENSO signal in the North Pacific (Hare & Mantua 2000, McGowan et al. 2003, King 2005, Checkley & Barth 2009). These climate-driven ecosystem regime shifts have induced fluctuations in anchovy spawning biomass, adult abundance, and recruitment (Chavez et al. 2003, Alheit et al. 2009, MacCall 2011, MacCall et al. 2016). Additionally, strong El Niño events, typically characterized by warmer water temperatures and a sharp decline in plankton biomass on an annual time scale, have induced a decrease in anchovy larval survival, juvenile growth, fecundity, and recruitment, as well as geographic shifts in their spawning grounds (Fiedler et al. 1986, Butler 1989, Fissel et al. 2011, MacCall 2011). From a fisheries standpoint, anchovy catches have been continuously low since the early 1980s and remained at very low levels during the 1990s (Alheit et al. 2009), following a regime of low recruitment and reduced spawning stock biomass (Fissel et al. 2011). Given the small annual catch levels, mechanisms unrelated to fishing seem likely to drive this decline (MacCall et al. 2016). Anchovy population biomass was consistently low during the 1990s, showed an increase during the 2000s, declined again by 2010, and has recently (since 2015) started to increase again (Thayer et al. 2017, Sydeman et al. 2020).

Identifying the key environmental factors driving recruitment success and variation in number of fish populations is complex because numerous processes act synergistically at various points in the life cycle (Houde 2008, Ganias 2014). Spatially explicit individual-based models (IBMs) are extensively used for exploring how environmental variability can affect fish distribution, growth, survival, and recruitment (Werner et al. 1996, Daewel et al. 2011, Xu et al. 2013, Petrik et al. 2015). IBMs have the advantage, compared to Eulerian approaches, of following the fate of distinct individuals and their exposure to abiotic and biotic conditions as they are transported and move within a dynamic and heterogeneous environment (DeAngelis & Grimm 2014, DeAngelis & Diaz 2019). Rose et al. (2015) developed an end-to-end model for anchovy and sardine in the CCS that coupled submodels for hydrodynamics, nitrogen-phytoplankton-zooplankton-detritus (NPZD) lower food web dynamics, individual-based fish population dynamics, and harvest. The coupled models successfully reproduced several observed characteristics of anchovy and sardine populations for 1965–2008. In a companion paper, Fiechter et al. (2015) used the same historical simulation to find potential correlations between bottom-up forcing (i.e. physical and biogeochemical conditions) and abundances at different life stages (i.e. egg, Age-0 [juvenile], adult) that could explain the causal relationship of observed anchovy and sardine population cycles with historical changes in the environment. Politikos et al. (2018) further analyzed the historical simulation to identify potential drivers of sardine recruitment by comparing model outputs of sardine growth, mortality, and reproduction for different years and time periods. Nishikawa et al. (2019) also analyzed the historical simulation and focused on the anchovy and sardine responses to the iconic 1976–1977 North Pacific regime shift. These studies formed a solid foundation for mechanistically analyzing the response of anchovy and sardine to changing environmental conditions in the CCS.

Using the same historical simulation (albeit updated) from the Rose et al. (2015) model, the objective of this paper is to further explore how changes in key abiotic (circulation, temperature) and biotic conditions (zooplankton) can influence dynamics of anchovy early life stages in the CCS. We repeated the historical simulation for 1965–2000 with a larger-domain grid to allow full realization of anchovy spatial shifts. Our analysis is particularly designed to isolate the effects of the well-documented ENSO years and 3 climate regimes in the North Pacific (King 2005, MacCall et al. 2005) on the spawning and nursery habitats, pre-recruit growth and survival, and ultimately recruitment of anchovy. We analyzed the historical simulation to formulate the general response of anchovy recruitment to warm versus cold conditions at annual and decadal scales and discuss some key model uncertainties. We discuss the modeling results based on the historical simulation until 2000 (that confirmed the general hypothesis of years of cooler temperatures and higher prey availability favoring anchovy; see Chavez et al. 2003) in light of the recent years of increasing anchovy under apparently warm conditions (Thompson et al. 2019, Sydeman et al. 2020).

2. MATERIALS AND METHODS

2.1. Overview of the end-to-end model

The end-to-end model of anchovy and sardine in the CCS by Rose et al. (2015) consists of 4 submodels: (1) the Regional Ocean Modeling System (ROMS, Shchepetkin & McWilliams 2005) to describe hydrodynamics; (2) the NEMURO NPZD model (North Pacific Ecosystem Model for Understanding Regional Oceanography, Kishi et al. 2007) to simulate lower trophic level dynamics; (3) an IBM to represent the full life cycles of anchovy and sardine; and (4) a fishing fleet model that imposed dynamic fishing mortality on the sardine population. Since anchovy harvest was low during most of our simulation period, we did not include the latter submodel for anchovy. The 4 submodels are fully coupled, with fish consumption of the IBM imposing predation mortality on zooplankton in the NEMURO NPZD model. The submodels have been extensively described in Rose et al. (2015) and are only briefly summarized here, focusing on anchovy and the aspects important for simulating and interpreting the influence of interannual and decadal changes in environmental conditions on anchovy recruitment. A schematic diagram of the fully coupled end-to-end model for anchovy can be seen in Fig. S1 in the Supplement at www.int-res.com/articles/suppl/m680p111_supp.pdf.

Previous analyses of the end-to-end model (Fiechter et al. 2015, Politikos et al. 2018, Nishikawa et al. 2019) showed that the ROMS-NEMURO coupled submodels predicted relatively realistic spatial maps of surface chlorophyll (phytoplankton) concentrations and adequately captured the vertical profiles of temperature, nitrate concentrations, and chlorophyll concentrations, as well as the magnitude of ENSO-related sea surface temperature signals. Analyses of the historical simulation (~1960 to 2008) showed that the fish IBM realistically represented the growth, mortality, movement, and reproduction of sardine and anchovy within the 3-dimensional ROMS-NEMURO grid and explored various aspects of the possible causes of their decadal-scale population cycles. Simulated biomasses of anchovy and sardine captured the magnitude of observed biomasses, but they showed much less inter-annual variation. The analysis of the historical simulation by Fiechter et al. (2015) showed that fluctuations in the anchovy population were associated with Age-1 growth (via Age-2 egg production) and prey availability, and that fluctuations in the sardine population were correlated with Age-0 survival and temperature.

2.2. ROMS and NEMURO submodels

The CCS configuration of ROMS assumed a horizontal resolution of 7 km, 42 terrain-following vertical layers, and a 900 s time step. Open boundaries were forced by 5 d averaged fields from the Simple Ocean Data Assimilation (Carton et al. 2000) reanalysis, and surface forcing was derived from the datasets for Common Ocean-Ice Reference Experiments (Large & Yeager 2009). The NEMURO NPZD submodel represents organisms as functional groups, separated according to their trophic role (i.e. producers, consumers) and subdivided according to their size. NEMURO follows nitrogen, silica, 2 phytoplankton groups (small phytoplankton [SP], large phytoplankton [LP]), and 3 zooplankton groups (small zooplankton [SZ], large zooplankton [LZ], predatory zooplankton [PZ]). Water velocities and temperature from ROMS and the concentrations of SZ, LZ, and PZ from NEMURO were used as inputs to the anchovy (and sardine) IBM. The historical simulation in Rose et al. (2015) was rerun here for 1965–2000 with the extended model domain, specifically adding grid cells for ROMS between 18°–50° N and 110°–140° W

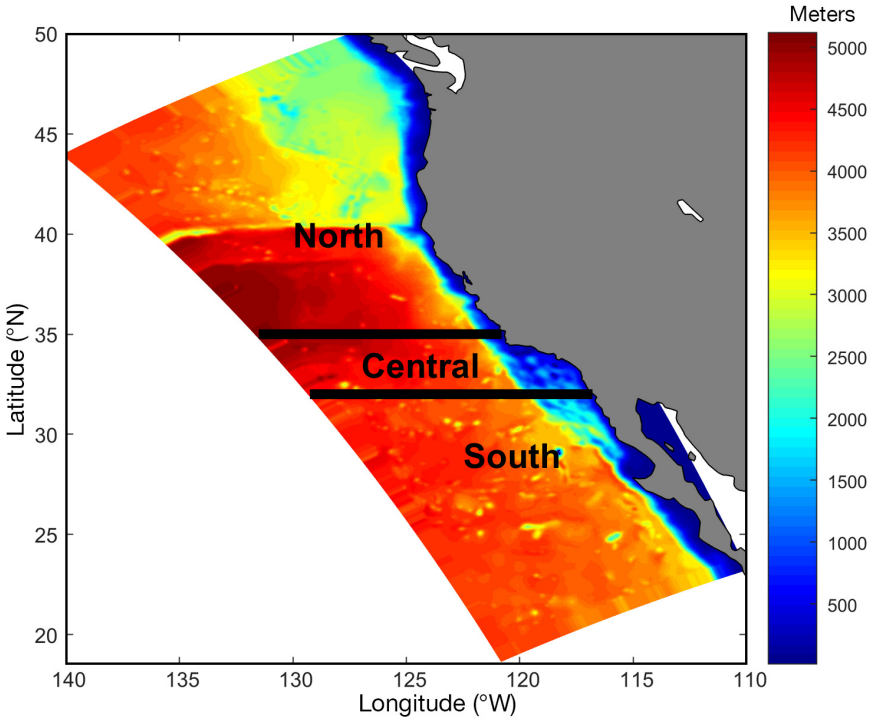

Fig. 1. California Current System model domain. Bathymetry in m. Black lines divide the domain into 3 subregions: south (south of 32° N), central (32°–35° N), and north (north of 35° N)

(Fig. 1). In some years, anchovy would concentrate near the southeast boundary of the original ROMS grid; the extended grid was designed to allow for their movement unconstrained by the domain boundary.

2.3. Individual-based anchovy model

2.3.1. Full life cycle

The IBM simulated the full life cycle dynamics of the anchovy and sardine populations by tracking individuals through 6 life stages: egg, yolk-sac larva, larva, juvenile, subadult, and adult. Key processes and parameters for the anchovy IBM are defined in Table 1. Eggs hatched into yolk-sac larvae that became larvae with the initiation of feeding; larvae metamorphosed to juveniles at 35 mm and juveniles became subadults (Age-1)

Table 1. Parameter values of key biological processes of anchovy in the individual-based model. Temp.: temperature

Process	Parameterization		Reference
Development	Metamorphosis (larvae to juveniles) at 35 mm		Hunter (1976)
	Egg & yolk-sac larva duration based on temp.: 4–7 d		Zweifel & Lasker (1976)
Consumption		Vulnerabilities (V_{SZ}, V_{LZ}, V_{PZ})	Rose et al. (2015)
	Larva	1.0, 0.5, 0	
	Juvenile	0.2, 1.0, 0.2	
	Subadult & adult	0.2, 0.4, 1.0	
		Optimal temperature range (°C)	Wang (1998), Okunishi et al. (2009)
	Larva	15–17	
	Juvenile	17–19	
	Subadult & adult	17–19	
Respiration		Reference temperature (°C)	Rose et al. (2015)
	Larva	15.5	
	Juvenile	17.0	
	Subadult & adult	17.0	
Mortality		Mortality (d^{-1})	Butler et al. (1993), Lo et al. (1995)
	Egg	0.23	
	Yolk-sac larva	0.16	
	Larva	0.128	
	Juvenile	0.009	
	Subadult & adult	0.002	
Movement	Optimal temperature: 14.0 °C		Lo et al. (2011)
Reproduction	Batch size: 260 eggs g^{-1} of fish		Butler et al. (1993)
	Spawning period: 1 Jan–1 May		Hunter & Macewicz (1980)
	Optimal temp. range for reproduction: 11.5–16.5 °C		Lluch-Belda et al. (1991), Lo et al. (2005)
	Resting time: 6–8 d		Rose et al. (2015)
	Number of batches: ~10–15		Rose et al. (2015)

on January 1. A fixed date termination of the juvenile stage was needed to start the annual age-class bookkeeping and to match the assumed birthdays in terms of empirical information. Subadult individuals became adults upon reaching maturity, which was length-dependent. Hourly feeding, growth, survival, and transport (egg, yolk-sac larva, larva) and behavioral movement (juvenile, subadult, adult) were computed for individuals.

The development of eggs within anchovy females and their release into the environment was dynamically represented through a rule-based approach, which focused on the reserves within the individual that were available for reproduction, the batch fecundity at subsequent releases, and the somatic condition of mature individuals. Once released, egg and yolk-sac larva development was temperature-dependent. Growth of larvae, juveniles, subadults, and adults was based on bioenergetics, with consumption dependent on the zooplankton biomasses generated by the NEMURO NPZD model. Mortality rate was stage-dependent for all stages, with added mortality due to starvation for feeding invidividuals. Egg, yolk-sac larva, and larva movement was simulated based on horizontal transport (particle-tracking algorithm) from ROMS, while the movement of juveniles, subadults, and adults was modelled using behavioral algorithms with temperature and zooplankton (food availability) as cues.

2.3.2. Growth

Hourly change in anchovy weight for larvae, juveniles, subadults, and adults was computed using the Wisconsin formulation for bioenergetics (Deslauriers et al. 2017), in which fish growth rate was defined as the difference between their consumption rate of zooplankton and the losses of energy due to respiration, egestion, excretion, and reproduction. Change in fish length was then calculated from weight, not allowing any loss in length. Consumption rate was an allometric function of weight, with a dome-shaped dependence on temperature. Assimilation efficiency (conversion of consumption into energy available to the individual) was assumed constant. Respiration rate was also weight- and temperature-dependent. Excretion and egestion were functions of consumption. Reproductive losses were based on the total number of eggs produced, assuming a fixed amount of energy loss for each released egg. The bioenergetics approach adapted from earlier models (Boggs 1991, Wang 1998, Urtizberea et al. 2008).

Determination of consumption rate was a multispecies functional response (Wang 1998) using 3 zooplankton types (SZ, LZ, and PZ) provided by the NEMURO model. Feeding preferences on SZ, LZ, and PZ were defined for each life stage considering specific vulnerabilities (ranging from 0 meaning no preference to 1 meaning full preference) based on feeding and diet studies (Sydeman et al. 2020), and half-saturation parameters determined the efficiency of anchovy feeding on the different zooplankton groups. As individual anchovy increased in size, their typical feeding activity favored larger zooplankton types (Hunter 1981, Lasker 1981). The feeding preference of each life stage is shown in Table 1. We assumed that larvae do not eat phytoplankton, although dinoflagellates may be a food source for early larvae (Scura & Jerde 1977, Sydeman et al. 2020). The phytoplankton groups represented in the NEMURO model were not sufficiently resolved to realistically represent dinoflagellates as prey for early anchovy larvae. Half-saturation constants were treated as calibrated parameters and were adjusted until simulated growth generated predicted weights-at-age that were similar to observed weights-at-age (Rose et al. 2015).

2.3.3. Mortality

Mortality of individuals was represented as natural mortality, starvation, and predation. Natural mortality rates were constant and specified for each life stage (Table 1). The duration of egg and yolk-sac larva stages was temperature-dependent; warmer temperatures shortened the duration of stages and consequently increased their stage-specific survival. Similarly, optimal temperatures and higher prey concentrations for larvae favored faster growth and thereby shortened their stage duration and increased their stage survival. Mortality due to starvation occurred when a fish weight dropped below 50% (for larvae) or 40% (for juveniles, subadults, and adults) of the expected weight calculated from fitted weight–length relationships (i.e. individuals became too skinny). Starved fish were removed from the simulation. Movement and consumption of individuals of a predator species (albacore) were simulated to impose a spatially variable predation mortality on anchovy. Predators were moved horizontally towards grid cells that maximized their growth rate (assumed feeding on anchovy and sardine) using

the restricted-area search approach (Rose et al. 2015). A predator individual then consumed anchovy in the horizontal cell for the entire water column. In the historical simulation, the contribution of albacore predation was relatively small compared to the prescribed natural mortality rate. Fishing mortality on anchovy was neglected due to small historical harvests, and thus the fishing fleet submodel was deactivated for anchovy in the historical simulation.

2.3.4. Reproduction

The annual spawning strategy of anchovy typically includes multiple batches whose precise number is dynamic and a function of both the fish's stored energy and current consumption rates (Hunter & Macewicz 1985a, Pecquerie et al. 2009). In the IBM, new eggs entered the anchovy population in multiple batches during an extended spawning period that lasted from 1 January to 1 May. A batch release from a mature individual was feasible when it experienced temperature within an optimal window and a resting time requirement between batches was satisfied, so that the individual was assured to have sufficient energy stored to release a new batch and atresia was not occurring (Hunter & Macewicz 1985b). Resting time was set to 1, meaning that the fish is ready to accumulate energy for spawning, and then was progressively reduced by the hourly development fraction of a fictitious batch until reaching zero, which indicated that a new batch could be started. Batch fecundity (number of eggs released per spawning event) of anchovies was weight- and consumption-dependent to allow for both capital and income spawning. The number of batches per spawner per season was variable, increasing when mature anchovies were experiencing good prey conditions and near-optimal temperatures for reproduction. Parameter values and their sources related to reproduction are listed in Table 1.

2.3.5. Movement

Anchovy were moved horizontally and vertically every hour in continuous space within the ROMS grid. Horizontal movement was determined by computing the velocities in the horizontal dimension (x and y) and updating the continuous location of each anchovy by adding to its location in each dimension the distance determined by the velocity times the 1 h time step. Velocities used for eggs, yolk-sac larvae, and larvae were the water velocities provided by ROMS to simulate passive transport. Temperature and prey biomasses were used as cues to determine the behavioral movement of juveniles, subadults, and adults using a kinesis algorithm (Humston et al. 2004, Watkins & Rose 2013). Velocities were based on assumed swim speeds and kinesis computes the x and y velocities (swim speeds) as a weighted sum of inertial (last time step) and random velocities. When an individual experienced unfavorable temperature and zooplankton conditions, the random component dominated, while the inertial component dominated during good conditions. Horizontal movement with kinesis appeared as individuals searching when conditions were bad and maintaining their direction and slowing down when conditions were good. Eggs and yolk-sac larvae were restricted to the top layer of the ROMS grid. After updating the horizontal movement, anchovy (all stages except eggs and yolk-sac larvae) were moved vertically towards the layer with the highest zooplankton levels within the water column; the water column was centered on the cell determined by the horizontal movement within the same time step.

2.3.6. Computational approach: super-individuals

To represent the anchovy population, we used the super-individual approach (Scheffer et al. 1995), because the many millions of individual anchovies in nature cannot be tracked separately in the model. All calculations of growth, mortality, reproduction, and movement were performed for each super-individual in the model and then scaled up to the population level. Each super-individual represents the 'worth' of some number of identical population individuals. The sum of worths over all super-individuals is the number of individuals at the population-level. New super-individuals were introduced through reproduction and assigned an initial worth based on that year's production of eggs accumulated over individuals and multiple batches throughout the spawning season. Mortality was represented by reducing the worth of the super-individual, while keeping the super-individual in the simulation. All output variables reported here have been adjusted for the worths of the super-individuals, so model results represent the population level. For example, mean length at recruitment was the weighted average length of recruits with the statistical weights being their worths and abundances are the summed worths.

2.4. Model analysis

All analyses were performed on the re-run of the 1965–2000 historical simulation. We compared anchovy dynamics for specific years (3 El Niño and 3 La Niña years) corresponding to extreme climate conditions and for the 36 years of the historical simulation divided into 3 well-documented decadal regime periods. Three model-to-data comparisons were performed to check key dynamics predicted by the model. We focus here on the analysis of extreme years and regimes within the historical simulation. We used 2 types of anomalies throughout the analysis. A difference anomaly ($Y - Y_{mean}$) was used when the focus of the comparison was on differences over time within a model output variable (Y); the difference anomaly is in the same units as the output variable, and the changes in anomaly values can therefore be interpreted relative to the magnitude of the variable. When we wanted to compare temporal patterns across multiple model output variables or with available empirical information (e.g. field data or derived from field data), we used the more familiar standardized anomaly $(Y - Y_{mean}) / Y_{SD}$.

2.4.1. *A priori* identification of ENSO years and regimes in the CCS

ENSO is a well-known mode of environmental variability that typically lasts 1 to 2 yr with different intensities and timing among years (McGowan et al. 2003, McClatchie 2014). El Niño episodes (the warmer phase of ENSO) are characterized by anomalously warm temperature and increased dynamic sea surface height, decreased primary and secondary productivity, and a deepening of the mixed layer (McClatchie 2014). In contrast, La Niña events (colder phase of ENSO) have opposite effects to El Niño (i.e. cooler temperature, increased productivity) (Murphree & Reynolds 1995). We focus on 3 well-known El Niño years (1983, 1992, and 1997/1998) and 3 well-known La Niña years (1975, 1989, 1999) that have been documented in the CCS (Simpson 1983, Hayward 1993, Lynn et al. 1995, Murphree & Reynolds 1995, Chavez 1996, Lynn & Bograd 2002, McClatchie 2014, http://ggweather.com/enso/oni.htm).

Specification of regimes is more subjective than extreme years, because multiple years and multiple response variables are involved, and the starting and ending years are debatable (Hare & Mantua 2000, Mantua 2004, Overland et al. 2008). Regime shifts in the North Pacific have been described for 1925, 1947, 1977, 1989, and 1998/1999 (Hare & Mantua 2000, King 2005). We divided our 1965–2000 simulation into 3 regimes bookended by these shifts: Regime 1 started in 1965 and ended in 1976, just before the 1977 shift; Regime 2 picked up in 1977 and ended in 1988, just before the 1989 shift; and Regime 3 went from 1989 to the end of the simulation in 2000. Based on analyses by others (Palacios et al. 2004, MacCall et al. 2005), Regime 1 was cool and had weak stratification, a shallow mixed-layer depth, and probably strong upwelling, resulting in a period of high primary and secondary productivity. Regime 2 was characterized by warmer and more stratified waters, weak upwelling (Checkley & Barth 2009), and a decline in zooplankton biomass (McGowan et al. 2003). Regime 3 was separated from the earlier warm regime (Regime 2) because a further shift in environmental components of the North Pacific ecosystem was documented (Hare & Mantua 2000).

We initially analyzed the temperature and zooplankton on the model grid for the general habitat of anchovy to confirm that temperature and zooplankton in the extreme years (3 warm and 3 cold) and 3 regime periods differed within the historical simulation. Given the inshore distribution of anchovies in the CCS, we quantified their annual environment by averaging temperatures and prey concentrations over the model domain for depths between 0 and 100 m.

2.4.2. Analysis of anchovy dynamics in historical simulation

We analyzed the model outputs for anchovy response to extreme years and regimes by starting with spawning and following the signals through eggs, larvae, and juveniles to recruitment at Age-1. All output variables used are listed in Table 2. For the analyses related to each life stage, we first examined the extreme years (comparing cold to warm years) and then compared among the 3 regimes (cold Regime 1 versus warmer Regimes 2 and 3). Comparisons were done for each extreme year, years viewed as either warm and cold, and for years (individually and averaged) within each regime.

We started with the simulated spawning habitats and the spatial distribution of eggs that are shown as the center of gravity (i.e. longitude and latitude) of annual egg production. We also computed the proportion of total egg production in each of the 3 horizontal bands classified as south (<32° N), central (32°–35° N), and north (>35° N) (Fig. 1). These 3 subregions were defined based on model-simulated dis-

Table 2. List of model output variables, including where used in figures and tables and how computed, extracted from the historical simulation and used to explore the effect of climate variation change on anchovy recruitment. Worth defines the number of identical population individuals represented by each super-individual

Output variable	Results	Computation from super-individuals
Annual egg production	Figs. 4 & 10, 12 as rec/eggs Fig. 5 as percent by subregion	Number of eggs released by each adult super-individual in every batch was multiplied by the worth of the super-individual at time of each release. Total annual egg production was then the sum of the total worth-adjusted eggs released over all adult super-individuals in multiple batches each year. The same calculations were done for egg production by subregion using the locations of super-individuals.
Recruitment (rec)	Figs. 3 & 9, 12 as rec/eggs	Sum of worths of juveniles on December 31.
Annual spatial distribution of eggs	Fig. 4	Worths of egg super-individuals at day of release were summed daily throughout the water column for each horizontal cell of the model grid. Daily total eggs in each cell were then averaged over the days in the spawning period of each year.
Mean longitude and latitude of organisms	Figs. 4, 11 & 12 (eggs)	Worths of super-individuals of each life stage were summed each day throughout the water column for each horizontal cell of the model grid. Using the center of each cell, the average longitude and latitude were then calculated over the grid cells using the summed worths of each cell. The resulting daily longitudes and latitudes were then averaged over the days in each year.
Adult anchovy spatial maps for cold and warm years	Fig. S2	Worths of adult super-individuals were summed daily throughout the water column for each horizontal cell of the model grid. Daily total adults in each cell were then averaged over the days in each year.
Temperature and zooplankton latitude-year	Fig. S3	On each year, annual average of temperature and zooplankton maps was computed on the water column over 0–30 m from the NEMURO model. Temperature and zooplankton were then averaged for each latitude level.
Spatial maps of temperature and zooplankton for cold and warm years	Figs. S4 & S5	Annual average of temperature and zooplankton on the water column over 0–30 m from the NEMURO model.
Annual reproductive potential (RP)	Figs. 6 & 11	The number of batches, spawning fraction, and batch fecundity were calculated daily for each mature super-individual throughout the water column for each horizontal cell of the model grid and then averaged over all super-individuals within a cell, using their worths as the weighting factor. Daily average values in each cell were then averaged over the days in each year, and their geometric mean is reported as RP. The same calculations were done for RP by subregion, using the locations of super-individuals.
Zooplankton where larvae are located	Figs. S6 & S7	On each day, the zooplankton concentration available to larval super-individuals were averaged for all super-individuals in a cell using the worths of the super-individuals as the weighting factor. The worth-adjusted daily zooplankton concentration available in each cell was then averaged over the days in each year.
Annual average temperature at egg release	Fig. 7	The temperature experienced by eggs at their release was averaged using the worth of the super-individual at release as the weighting factor. Daily experienced temperatures were then averaged for each year.
Annual stage survival (fraction)	Figs. 7 & 11 (eggs, yolk-sac larvae), Figs. 8 & 11 (larvae)	Worth of each super-individual upon entering and exiting a life stage was used to compute the fraction surviving. Annual survival was the average fractions over all super-individuals of the same life stage weighted by their worth when entering the life stage.
Annual consumption rate	Fig. 7 (larvae), Fig. 7 (juveniles)	Consumption rate (expressed through P-values) was averaged daily using the worth of the super-individual as the weighting factor. Daily P-values were then averaged over the days in the year.
Proportion recruitment from subregions	Table 4	Summed worths of juvenile super-individuals on December 31 in their subregion where they recruited divided by the total sum of worths of all recruits for that year.
Annual length of recruits	Figs. 8 & 11	Average length of juveniles on December 31, using their worth on December 31 as a weighting factor.

tributions of eggs to highlight differences in model results (e.g. south versus central) and do not exactly match divisions of the spatial domain used by others (e.g. Checkley & Barth 2009). The central subregion covers the core area of the California Cooperative Oceanic Fisheries Investigations survey program (Bograd et al. 2003, Gallo et al. 2019, see also www.calcofi.org). We report the annual anomaly (value minus overall mean for the 36 yr) of proportion of eggs produced in each subregion for each year.

To further decipher the extreme year and regime differences on reproduction, we summarized reproduction each year using several indices derived from model outputs. We characterized the annual spawning behavior and performance of mature anchovies by the total number of batches per mature individual, spawning fraction (which computes the proportion of the female population that released eggs daily), and the batch fecundity (which gives the number of eggs released per individual in a single spawning event). Annual values of these 3 variables for all spawners were computed (Table 2), and we report their geometric mean as a composite index of reproductive potential (RP). Annual anomalies of RP (values minus overall average) are shown for the southern, central, and northern subregions.

After spawning, we examined eggs and yolk-sac larvae. For each year, we computed the average temperature of egg release and the fraction of eggs that survived to larval stage (i.e. from release through egg and yolk-sac larva). As with the other variables, we report annual anomalies based on subtracting the overall mean value from each year's value.

For larvae and juveniles, we focused on stage survival, zooplankton availability, and growth (Table 2). The proportion of maximum fish consumption (called P-value in bioenergetics literature) was used to describe changes in consumption rates of anchovy. The P-value combines the concentrations of the 3 zooplankton groups (SZ, LZ, and PZ), weighted by the stage-specific vulnerabilities and foraging efficiencies, and ranges between 0 (no feeding) and 1 (high feeding, Rose et al. 2015). Averaged annual P-values were computed for larvae (Table 2). Finally, annual larval stage survival was computed (Table 2). All larval outputs are shown as annual difference anomalies.

A subset of the output variables for larvae was computed for juveniles. The juvenile stage ended at recruitment to the subadult stage (December 31), and recruitment was the sum of juvenile worths on December 31 (Table 2). The mean length of recruits was recorded for each year, using their worth as weighting factor. Juvenile stage survival was defined as the fraction of larvae surviving from juvenile metamorphosis to recruitment. We therefore examined the annual ratio of annual recruitment to total egg production (rec/eggs) as an indicator of recruitment success. All juvenile outputs (except mean length) are shown as annual anomalies.

All anomalies used here, except for rec/eggs, are the difference between a year's value and the averaged value. We used standardized anomalies for rec/eggs because we compare it later to field-derived values. For both difference and standardized anomalies, we also report the average of the difference anomalies by regime (R_1, R_2, and R_3) and the percent change in these averaged values (ΔR) from Regime 2 to 1 and from Regime 3 to 2 (e.g. $\Delta R_{1,2} = [R_2 - R_1]/R_1 \times 100$).

2.4.3. Selected model comparisons

We performed 3 direct comparisons of model outputs to available empirical information in the CCS. Many other aspects of the model simulation were qualitatively evaluated for the present analysis (rerun of the historical simulation) and in earlier papers (Fiechter et al. 2015, Rose et al. 2015, Politikos et al. 2018, Nishikawa et al. 2019). The first formal comparison reported here involved the ratio of recruitment to spawning stock biomass (rec/SSB) and recruitment success (rec/eggs) that served as our primary response variables for subsequent analyses. Annual estimates of SSB and recruitment based on stock assessment and recruitment models are available (Jacobson et al. 1995, Fissel et al. 2011). Predicted and empirically estimated standardized anomalies of annual rec/SSB were compared with time series plots and with percent changes in average rec/SSB between Regimes 2 and 1 and between Regimes 3 and 2. As a check whether similar results would be obtained using total number of eggs rather than SSB, we also compared model-predicted and estimated rec/eggs, which was available for 1981–2000 (Fissel et al. 2011). We used Fissel et al. (2011) for model evaluation, although more recent SSB estimations are available (Thayer et al. 2017), because we wanted to use a single source to ensure consistency for the rec/SSB and rec/eggs values.

The second and third comparisons focused on 2 aspects of model results (spatial shift in eggs, larval growth) that were consistently highly important in explaining differences in rec/eggs among the warm and cold years and among the 3 regimes. We compared the latitudinal centers of simulated egg distri-

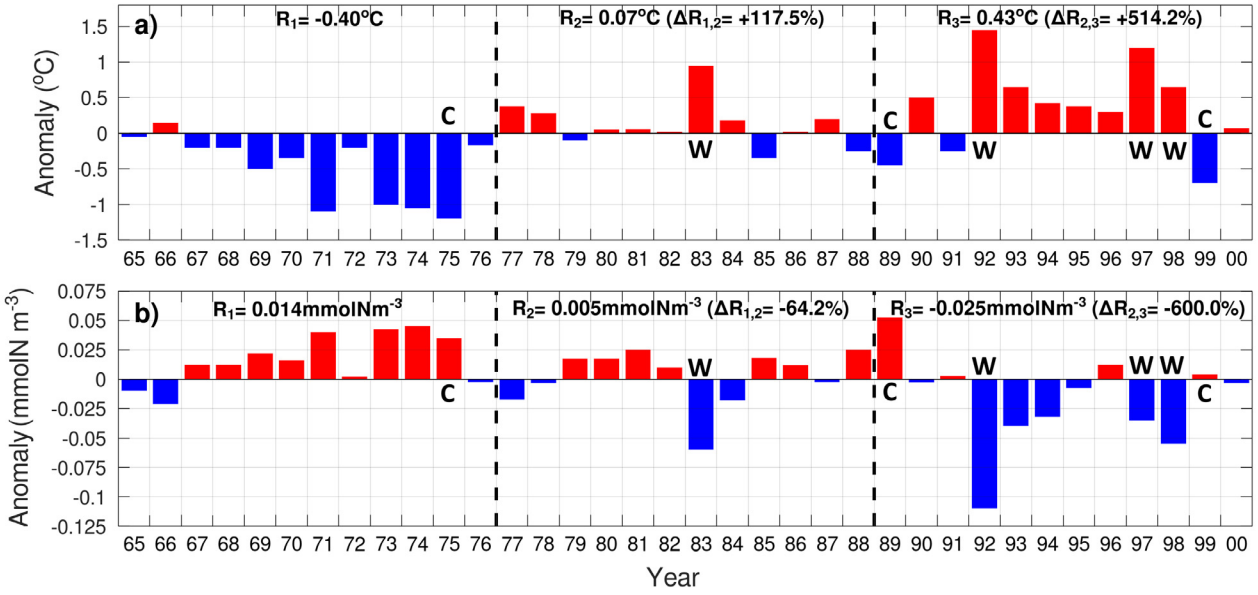

Fig. 2. Average annual difference anomalies of upper water column (0–10 m) for (a) temperature and (b) total zooplankton (SZ, LZ, and PZ) over 1965–2000, as predicted from ROMS-NEMURO submodels. Anomalies (red: positive, blue: negative) were calculated by removing the 1965–2000 mean from each annual value. Dashed lines separate the 1965–2000 period into 3 regime periods: Regime 1 (R_1: 1965–1976), Regime 2 (R_2: 1977–1988), and Regime 3 (R_3: 1989–2000). Averaged anomalies for each regime and percent changes are shown ($\Delta R_{1,2}$: R_2 compared to R_1) and ($\Delta R_{2,3}$: R_3 compared to R_2). C and W: cold (La Niña) and warm (El Niño) extreme years within the historical simulation, respectively

butions with the latitudinal centers of eggs computed from the CalCOFI sample stations within the 30°–35° N core sample area. We also compared the simulated larval consumption rate with the annual volume of small zooplankton measured in the CalCOFI program (Bograd et al. 2003, Gallo et al. 2019).

2.4.4. Synthesis

We summarized the extreme year and regime comparisons by comparing the responses across output variables of warm versus cold years with the responses for the cold Regime 1 to warmer Regimes 2 and 3 (i.e. effect of warm conditions). We used standardized anomalies to highlight the temporal patterns across variables. The correlations between annual anomalies and rec/eggs are summarized in Table 3.

3. RESULTS

3.1. Anchovy environment: temperature and zooplankton

Temperature and zooplankton conditions in which anchovies are generally found (<1000 m depth) on the model grid showed consistent differences between the warm (El Niño) and cold (La Niña) years and among the 3 regimes (Fig. 2). Positive temperature anomalies (relative to the average) occurred during the warm years 1983 (+0.98°C), 1992 (+1.48°C), late 1997 (+1.19°C) and 1998 (+0.65°C) (Fig. 2a). In contrast, negative temperature anomalies occurred for the cold years 1975 (–1.16°C), 1989 (–0.48°C), and 1999 (–0.63°C) (Fig. 2a). When the anomalies were averaged across years by regime, they showed Regime 1 was the coldest (–0.40°C), Regime 2 was slightly warmer (+0.07°C), and Regime 3 was the warmest (+0.43°C). Percent changes in averaged anomalies were large for Regime 2 to 1 and for Regime 3 to 2 (>100 % for both).

Variation in total zooplankton concentration for the same coast-associated habitat aligned with the temperature anomalies (Fig. 2b). Negative anomalies in total zooplankton (SZ, LZ, and PZ) biomass occurred during the warm years 1983 (–0.06 mmolN m^{-3}), 1992 (–0.11 mmolN m^{-3}), late 1997 (–0.04 mmolN m^{-3}), and early 1998 (–0.05 mmolN m^{-3}). Conversely, positive zooplankton anomalies occurred in the cold years 1975 (+0.03mmolN m^{-3}), 1989 (+0.05), and 1999 (+0.005). On the decadal scale, the average zooplankton anomalies by regime were highest in Regime 1 (+0.014 mmolN m^{-3}), decreased (but still positive) in Regime 2 (+0.005), and reached a low in

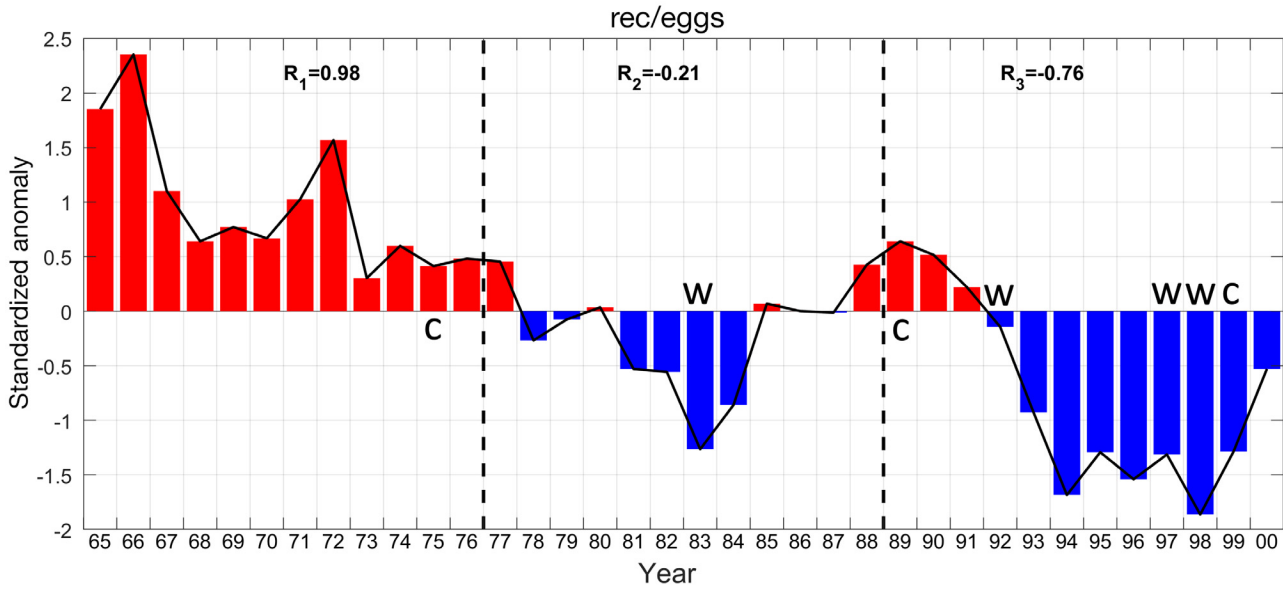

Fig. 3. Standardized anomalies of annual anchovy recruitment success (ratio of recruitment to total egg production) shown as time series (black line) and bars for the 1965–2000 simulation time period. Anomaly was computed as value minus overall mean for 1965–2000 and divided by the standard deviation across all years. The averaged anomalies are indicated for each regime (R_1, R_2, and R_3). C and W: cold (La Niña) and warm (El Niño) extreme years within the historical simulation, respectively

Regime 3 (−0.025). Differences on a percent change basis between Regime 2 versus 1 and Regime 3 versus 2 were large (>50% for both).

3.2. Simulated recruitment success

Our primary response variable of annual recruitment success (rec/eggs) in the historical simulation showed a declining trend (Fig. 3). Recruitment success was lower in warm (rec/eggs = 4.27×10^{-4} to 6.77×10^{-4}) versus the cold years 1975 (7.58×10^{-4}) and 1989 (7.91×10^{-4}). The corresponding standardized anomalies were −1.44 to 0.0425 for warm years and 0.413 and 0.64 for the cold years 1975 and 1989, respectively. The cold year of 1999 was an exception with low rec/eggs (5.11×10^{-4}, standardized anomaly of −1.29), similar to the warm years. When averaged over years within each regime, rec/eggs was highest in the colder Regime 1 (8.41×10^{-4}; standardized anomaly of 0.98) compared to Regimes 2 (6.67×10^{-4}; standardized anomaly of −0.21) and 3 (5.86×10^{-4}; standardized anomaly of −0.76).

3.3. Latitudinal shifts in spawning habitats

Spatiotemporal changes in environmental conditions during ENSO events and the regimes shifted the geographic ranges of anchovy spawning habitat. In the warmer years of 1983 and 1998, simulated egg abundance distributions extended into the northern subregion (>35° N), whereas the colder years of 1975 and 1989 favored spawning activity in the central and southern subregion <34° N) (Fig. 4). The remaining warm (1992) and cold (1999) years had similar egg abundance distributions, roughly centered on 36° N. Among regimes, the proportion of eggs released in the northern subregion increased (Fig. 5), resulting in a northward shift of spawning from 33.1° N in Regime 1 to 35.2° N in Regime 2 and to 35.8° N in Regime 3. Averaged over years within regimes (Fig. 5), anomalies of the percentage of eggs by subregion went from negative in the north (−19.6) and positive in the south (+13.3) in Regime 1 to positive in the north (R_2 = 3.6, R_3 = 19.2) and negative in the south (R_2 = −4.3, R_3 = −10.5) in Regimes 2 and 3. Across all years, the latitudinal shifts of egg distribution were inversely correlated to recruitment success (r = −0.8, $p < 0.001$) (Table 3).

The effect of temperature on the success of adult anchovy spawning was the underlying mechanism that determined the shifts in egg distributions. Some movement in response to temperature (and to a lesser extent zooplankton) also contributed to the northward shift of adults (see Fig. S2 in the Supplement). Warm conditions during the years of 1983, 1992, and 1998 shifted the preferred temperature range for reproduction (11.5–16.5°C) to the north (Fig. 4, black isotherms). This induced an increased

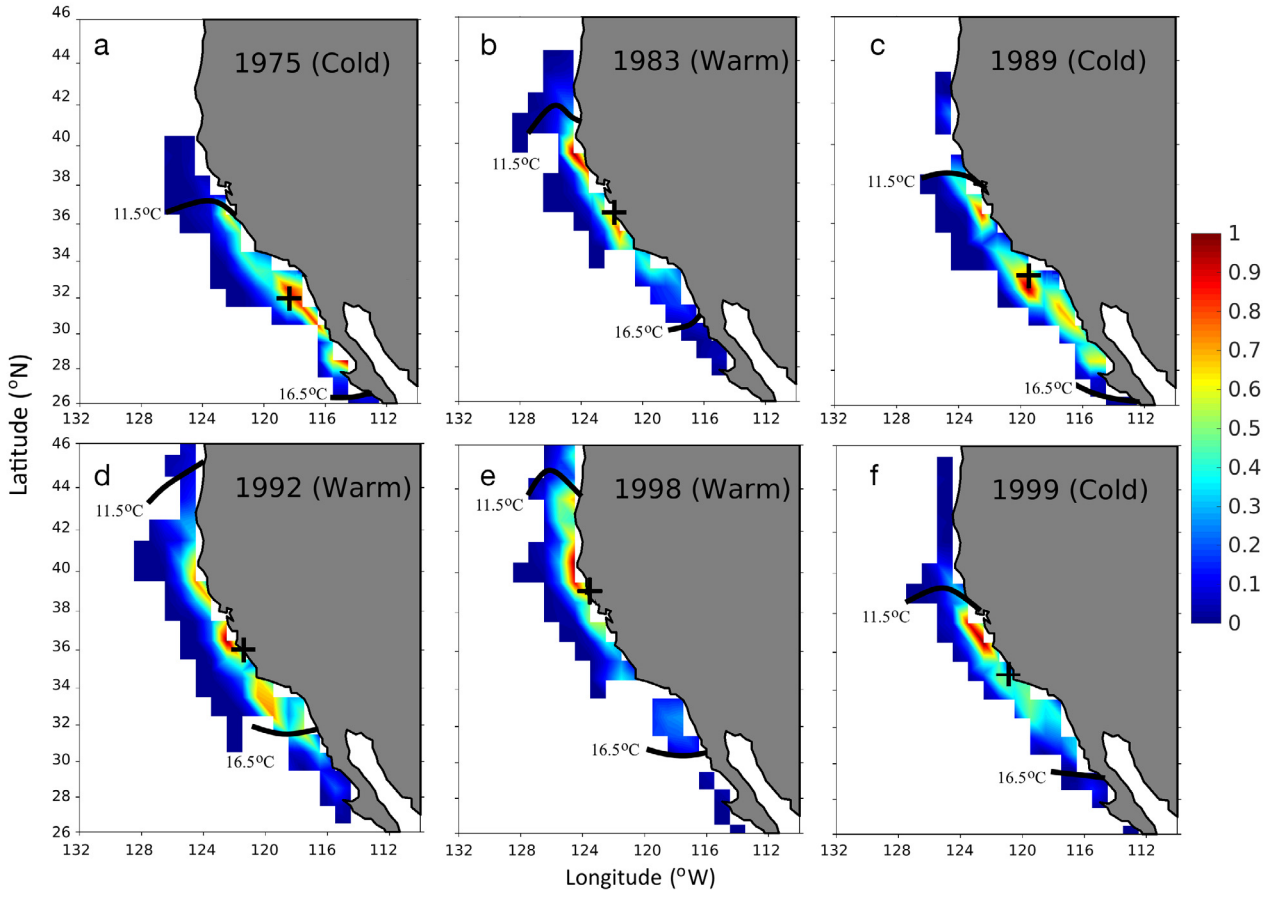

Fig. 4. Averaged anchovy egg abundance distributions for (a,c,f) cold years (1975, 1989, 1999) and (b,d,e) warm years (1983, 1992, 1998). Grid cells of the maps were normalized to a scale of 0–1 for each year separately, using the formula: $X_{norm,cell} = (X_{cell} - \min X_{all\text{-}cells})/(\max X_{all\text{-}cells} - \min X_{all\text{-}cells})$. (+) Center of gravity (longitude, latitude) of egg distributions. Black lines: 11.5 and 16.5°C isotherms for the range of reproduction temperatures

number of batches and spawning fraction for anchovies found in the northern subregion (>35° N), ultimately resulting in the increase of their RP for warm years (Fig. 6a). Concurrently, the RP of anchovies found in the southern subregion (<32° N) declined significantly in 1983, 1992, and 1998 (Fig. 6c). In contrast, the colder winter temperatures of 1975, 1989, and 1999 caused a noticeable decrease in the number of batches and spawning fraction in the northern subregion. As a result, the RP in the cold years declined in the northern subregion (Fig. 6a) and increased in the southern subregion (Fig. 6c).

On the regime scale, the RP of anchovies found in the northern subregion generally shifted from negative anomalies in Regime 1 to positive anomalies in Regimes 2 and 3 (Fig. 6a). As with the proportion of eggs, averaged anomalies went from negative in the north (−0.102) and positive in the south (+0.041) in Regime 1 to positive in the north (R_2 = +0.062, R_3 = +0.053) and negative in the south (R_2 = −0.014, R_3 = −0.033) in Regimes 2 and 3. In the northern subregion, these anomalies corresponded to a 160.7% increase from Regime 2 to 1 and a 14.5% decrease from Regime 3 to 2, which was still an increase in Regime 3 relative to Regime 1. A strong negative correlation (r = −0.78, $p < 0.001$) of RP (over years) occurred between the northern and southern subregion. The underlying mechanism for the northward shift in spawning was a combination of the increased success of spawning in the north and, to a lesser degree, the within-year movement of adults in response to temperature and zooplankton. Temperature and zooplankton groups showed very clear year-to-year differences and little evidence of clear south-to-north shifts in warm years or regimes (see Figs. S3–S5 in the Supplement). This suggests that both differential reproductive success and movement farther north were important. Without some contribution from movement, northward shifts in warm years would not be possible. The northward move-

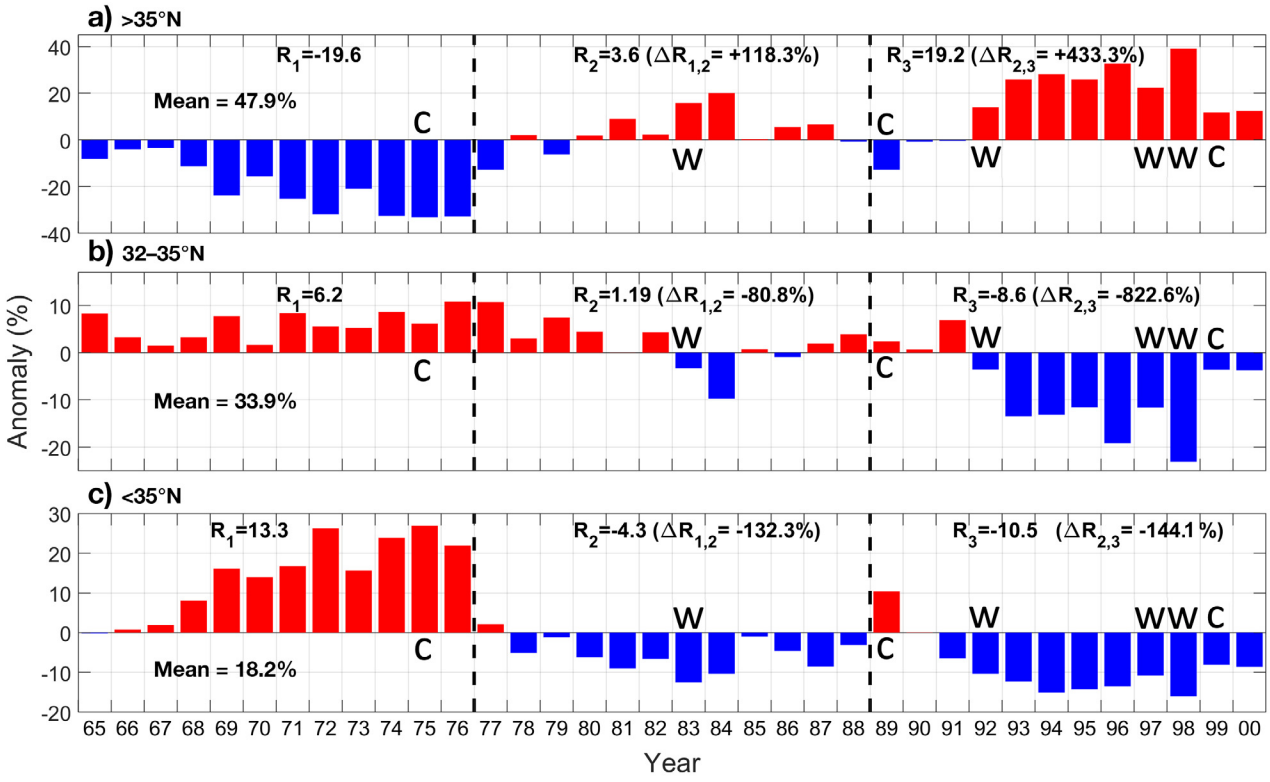

Fig. 5. Annual difference anomalies of the percent of anchovy eggs released in the (a) northern, (b) central, and (c) southern subregions (see Fig. 1) during 1965–2000. Anomalies were computed by subtracting the 1965–2000 mean (shown on each panel to help in the interpretation of the magnitude of the anomalies). See Fig. 2 for definitions of R_1–R_3, $\Delta R_{1,2}$, $\Delta R_{2,3}$, C, and W

Table 3. Correlations (r) of annual values of model variables related to egg and yolk-sac larvae, larvae, and juveniles with annual simulated recruitment success (recruitment per no. of eggs)

Variable	r
Reproductive potential (north)	−0.37
Reproductive potential (central)	−0.19
Reproductive potential (south)	+0.47
Temperature of egg releases	+0.58
Egg and yolk-sac larval survival	+0.62
Larval consumption	+0.75
Larval survival	+0.76
Juvenile consumption	−0.25
Length of recruits	+0.35

ments were in response to temperature, with the patchier zooplankton playing a secondary role.

Across all years, the decline of RP in the southern subregion aligned with the decline in recruitment success (r = 0.47, p = 0.011), whereas the increase of RP in the northern subregion was inversely correlated to recruitment success (r = −0.37, p = 0.014) (Table 3). The low correlation for the central subregion (r = −0.19, p = 0.02) reflected that relatively constant spawning occurred year-to-year in that subregion.

3.4. Egg and yolk-sac larva survival

Changes in temperature imposed interannual and decadal-scale fluctuations in egg and yolk-sac larva (EYS) survival. In 1992, the temperature anomaly during egg releases was +0.65°C (Fig. 7a), resulting in a reduced EYS stage duration (mean ± SD of 6.9 ± 2 d) and an EYS survival anomaly of +2.12% (Fig. 7b). In contrast, the cooler conditions during egg releases in 1999 (anomaly of −0.61°C, Fig. 7a) increased EYS duration (mean of 7.6 d) and lowered the EYS survival (anomaly of −3.4%, Fig. 7b). Egg survival showed a significant positive correlation with recruitment success (r = 0.62, p < 0.001) (Table 3).

However, the effects of the other warm and cold years on temperature experienced by eggs and EYS survival were not consistent. Despite the highly contrasting signs of temperature anomalies over the model domain between 1983 (positive) and 1989 (negative, Fig. 2a), egg-experienced temperatures were near the 35 yr average (i.e. small anomalies of +0.08°C in 1983 and −0.05°C in 1989, Fig. 7a). This resulted in similar EYS stage durations between 1983 (mean of 7.8 d) and 1989 (mean of 7.4 d), and, in turn, similar anomalies in EYS survival (+0.06% in 1983

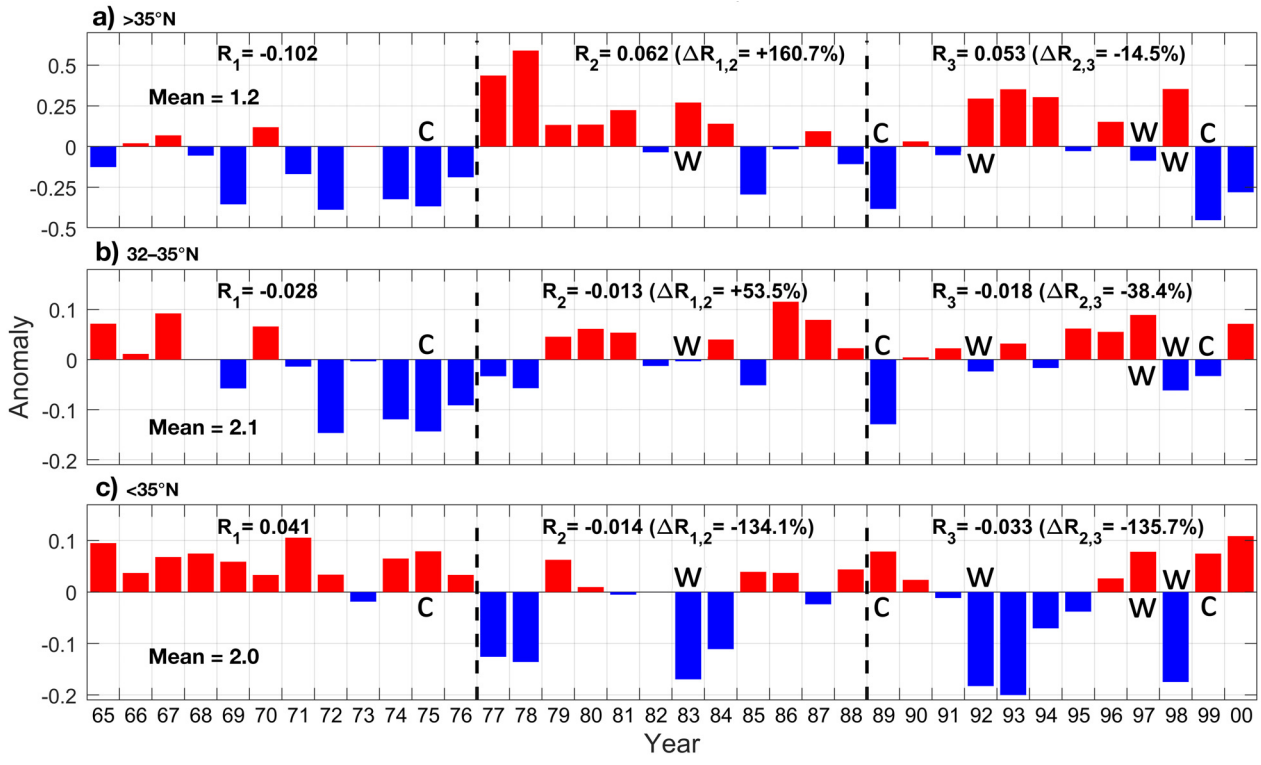

Fig. 6. As in Fig. 5 but for reproductive potential (RP), calculated as the geometric mean of annual number of batches, annual spawning fraction, and annual batch fecundity

and +0.44% in 1989, Fig. 7b). The remaining 2 years demonstrated that environmental conditions are not simply reflected in the simulated anchovy. Despite the warmer conditions in 1998 (Fig. 2a), the temperature anomaly at egg release (–0.73°C) and the EYS survival anomaly (–2.9%) were negative (Fig. 7a,b). The year 1975 was one of the coldest years (Fig. 2a), but temperature anomalies experienced and EYS survival anomalies were slightly below zero.

As with extreme years, the consequences of shifted spawning had complicated effects on the temperature experienced by eggs and EYS survival among the regimes. Despite the warming trend in temperature in the model domain (Fig. 2a), eggs encountered progressively cooler temperatures in the different regimes (R_1: +0.18°C, R_2: +0.07°C, and R_3: –0.23°C, Fig. 7a). As a result, EYS survival anomalies declined from +0.75% in Regime 1 to +0.24% in Regime 2 (a 68% decrease) and to –0.96% in Regime 3 (a 500% decrease from Regime 2) (Fig. 7b).

3.5. Zooplankton and larval survival

Interannual and decadal-scale variation in zooplankton concentrations influenced larval growth and therefore also larval survival because larvae transitioned to juveniles based on their length. Negative anomalies in the sum of SZ and LZ (main prey for larvae) where larvae were located occurred in the warm years 1983, 1992, and 1998 (Fig. S6 in the Supplement). Inter-annual differences reflected the general overall changes in zooplankton throughout the grid; larvae were moved horizontally by physical transport and thus did not move horizontally in response to temperature or food. This reduced their consumption rates, which also showed negative anomalies (–0.02 in 1983, –0.04 in 1992, –0.034 in 1998, Fig. 7c). While the changes in the consumption rates were small, they were ecologically meaningful, because P-values get compounded every 900 s (time resolution of the IBM) for the duration of the life stage. Slowed growth resulted in longer stage durations and caused decreased larval stage survival relative to the 1965–2000 average (–0.017% in 1983, –0.015% in 1992 and –0.008% in 1998, Fig. 7d). Conversely, in 2 of the cold years (1975 and 1999), larvae experienced increased SZ and LZ concentrations. This resulted in higher consumption rates (Fig. 7c) and increased larval stage survival (+0.01% in 1975 and +0.007% in 1999, Fig. 7d). The remaining cold year (1989) showed higher zooplankton concentrations, similar to the other 2 cold years, but a larval survival anomaly that was close to zero (–0.0003%).

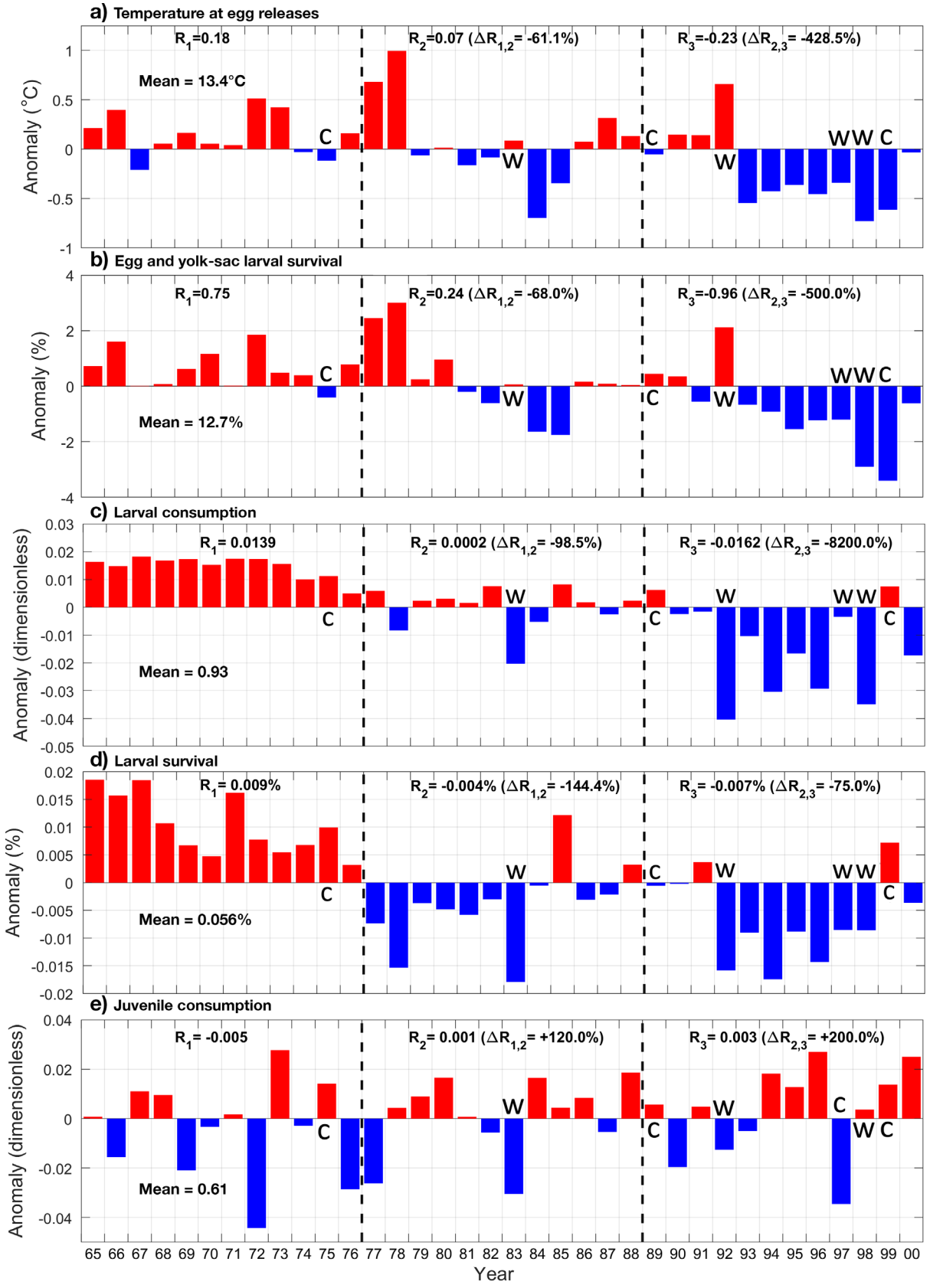

Fig. 7. Annual difference anomalies of (a) average temperature at anchovy egg releases, (b) % egg and yolk-sac larva survival, (c) larval consumption rate (dimensionless), (d) % larval survival, and (e) consumption rate (expressed through P-value, dimensionless) of juvenile anchovies during 1965–2000. See Fig. 2 for definitions of R_1–R_3, $\Delta R_{1,2}$, $\Delta R_{2,3}$, C, and W. Egg and yolk-sac larva stages were treated as 1 stage to define cumulative survival from egg to first-feeding larval stage

On the regime scale, the averaged zooplankton anomalies experienced by larvae (sum of SZ and LZ) turned from positive in Regime 1 to negative in Regime 2 within 34–38° N, and then negative south of 38° N in Regime 3 (Fig. S7 in the Supplement). Larval consumption rate declined from an anomaly of +0.0139 in Regime 1 to +0.0002 in Regime 2 and −0.0162 in Regime 3 (Fig. 7c), leading to a declining trend in larval stage survival from +0.009% in Regime 1 to −0.004% in Regime 2 and −0.007% in Regime 3 (Fig. 7d). The apparently small changes in larval survival are important, because they are large relative to the small magnitude of survival (i.e. $\Delta R_{1,2}$ and $\Delta R_{2,3}$ were large) and the sensitivity of model dynamics to larval stage survival. Larval survival also showed significant correlation with recruitment success ($r = 0.76$, $p < 0.001$) (Table 3).

3.6. Spatial distribution of recruits

The spatial extent of recruits also varied markedly between warm and cold years and regimes. Higher proportions of recruits were predicted in the northern subregion during the warmer years 1983 (50.5%), 1992 (55.2%), and 1998 (58.2%) with respect to the model domain (Table 4). Conversely, during the colder years 1975, 1989, and 1999, higher proportions of recruits were located south of 32° N (52.5% in 1975, 43.3% in 1989, and 34.3% in 1999), and the center of gravity of their distribution was located from 32.8° to 34.1° N. The central subregion (32°–35° N) retained a population of recruits, varying from 22.6 to 42.3%. Among the 3 regimes, the core of the recruits' distribution was concentrated between 28° and 32° N in Regime 1, whereas in Regime 2, their distribution decreased south of 32° N and increased considerably between 34° and 40° N. Regime 3 showed a small but continued movement north: the main core of recruit distribution was between 35° and 40° N and slightly decreased south of 34° N compared to Regime 2.

Table 4. Proportion of recruits (calculated as percentage of total) that recruited in the southern (<32° N), central (32°–35° N) and northern (>35° N) subregions of the model domain during warm and cold years. Gray shading: highest percent of recruits across the 3 subregions for each year

Year	South	Central	North
1975 (cold)	52	34	14
1983 (warm)	21	28	51
1989 (cold)	43	29	28
1992 (warm)	15	30	55
1998 (warm)	19	23	58
1999 (cold)	34	43	23

3.7. Growth of recruits

Lowered zooplankton conditions during the warm years of 1983, 1992, and 1997 caused a decreased consumption rate of juveniles (<−0.03, Fig. 7e) resulting in a smaller mean length at recruitment (~67 mm; Fig. 8). In contrast, juveniles had faster growth (mean length > 75mm) in the cold years of 1975, 1989, and 1999 (Fig. 8) because of more favorable prey conditions that increased their consumption rates (Fig. 7e). On a regime scale, the changes in consumption rates were sufficient in magnitude to result in a moderate decrease in the mean length of recruits among regimes: R_1 = 88.2 mm, R_2 = 77.5 mm, R_3 = 74.6 mm (Fig. 8). A positive correlation was found between recruitment success and length of recruits ($r = 0.35$, $p < 0.0005$) (Table 3).

3.8. Comparisons of model output to available empirical data

Model agreement with data-estimated rec/SSB was inconsistent. While the model-generated values showed a clear downward trend, the observed rec/SSB varied, but without a clear trend (Fig. 9a). There was no clear agreement when viewed on a year-by-year basis. The averaged standardized anomalies of rec/SSB were somewhat higher in the 3 cold years compared to the 3 warm years for the model (−0.6 versus −0.76) and also the empirically derived values (0.073 versus −0.725). The large negative value for 1999 for the simulation (−2.27) reduced the average for the model simulated cold years. There was a slight declining trend in estimated rec/SSB across the regimes. The averaged standardized anomaly values by regime showed a steady decrease in the model simulation (R_1 = 1.06, R_2 = −0.14, R_3 = −0.91), and the empirically estimated averaged anomalies also showed a decrease but less dramatic (R_1 = 0.23, R_2 = −0.13, R_3 = −0.25, Fig. 9a). When we used the more recent estimates of total eggs (rather than SSB) and recruitment (Fig. 9b), predicted recruitment success (rec/eggs) for years with empirical estimates during Regime 2 (1981–1988) versus Regime 3 showed a decrease (−0.34 to −0.76), and the empirical values also showed a decline (0.71 to −0.47).

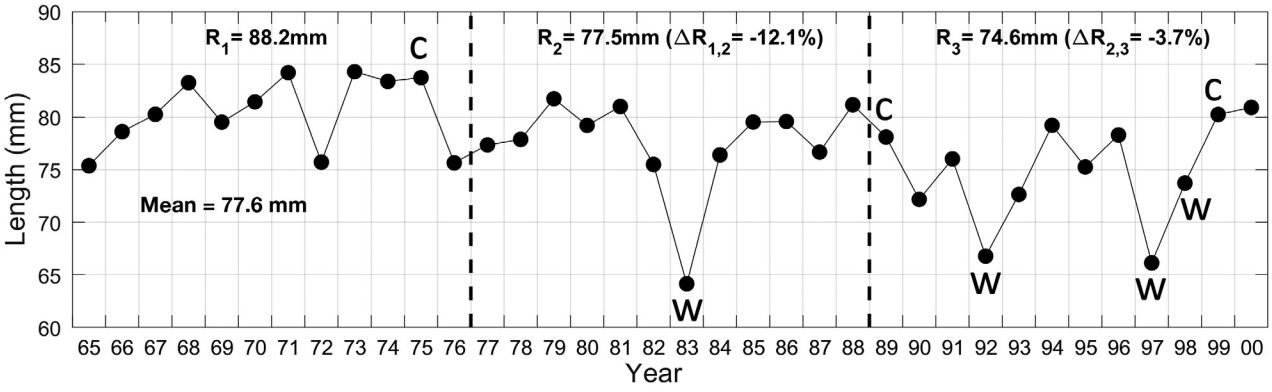

Fig. 8. Annual length of anchovy recruits during 1965–2000. See Fig. 2 for definitions of R_1–R_3, $\Delta R_{1,2}$, $\Delta R_{2,3}$, C, and W

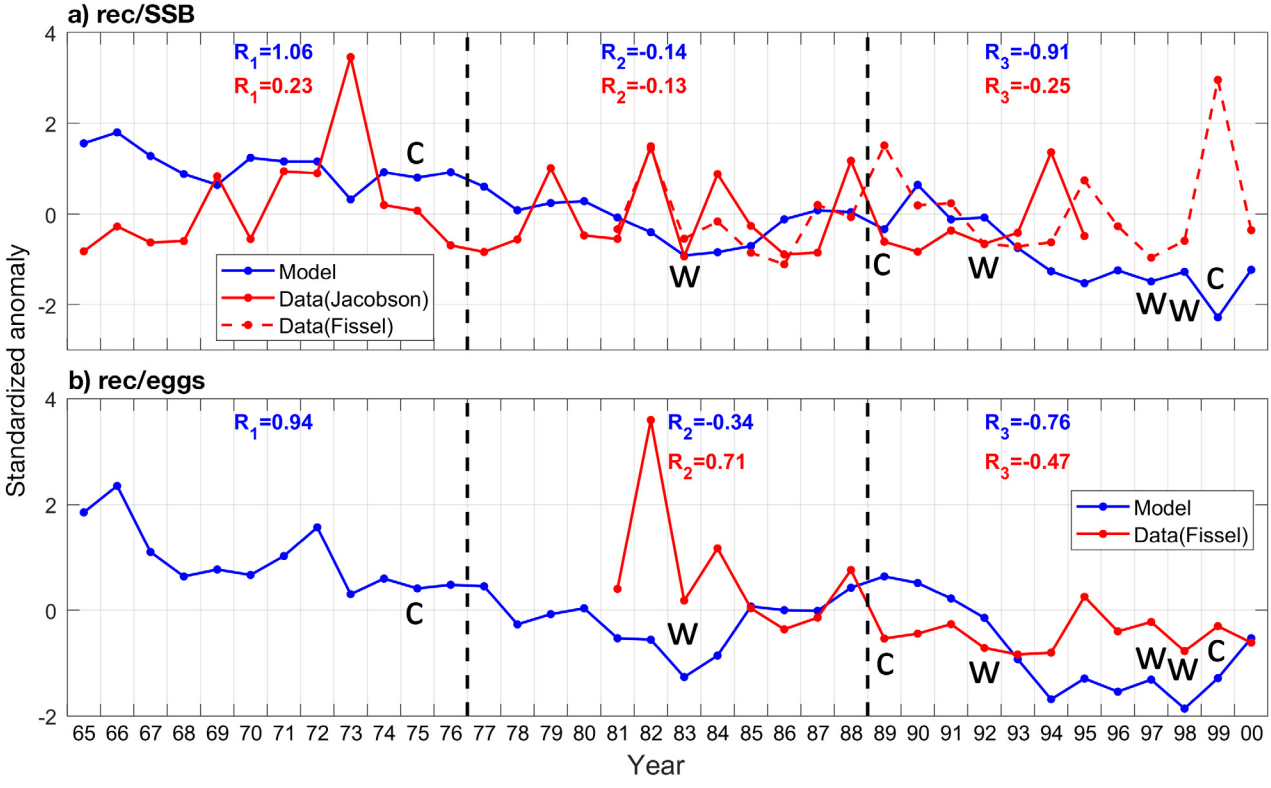

Fig. 9. (a) Time series of simulated (blue dots) and data-estimated (red dots) standardized anomalies $(Y - Y_{mean})/Y_{SD}$ of the ratio of recruitment to spawning stock biomass (rec/SSB) during 1965–2000 and (b) time series of simulated (blue dots) and data-estimated (red dots) anomalies of recruitment success (rec/eggs). Estimated rec/SSB values were derived from recruitment and stock assessment estimates reported in Fissel et al. (2011) and Jacobson et al. (1995), and estimated values of rec/eggs were available for 1981–2000 (Fissel et al. 2011). The averaged regime anomalies (R_1, R_2, and R_3) were calculated for simulated and data-estimated values for each regime

Both simulated and empirically based estimates of latitudinal centers of annual egg distributions showed increasing trends (Fig. 10a). Averaged latitude for the 3 cold years was 33.3° N in the simulation and 32.8° N in the empirical data; for the 3 warm years, the averaged latitudes were 37.1° N (simulated) and 33.6° N (empirical). Similar agreement was seen when annual latitudes were averaged for the simulation and empirical data by regime: 33.1° versus 32.6° N for Regime 1, 35.2 versus 32.9° N for Regime 2, and 35.8° versus 33.6° N (Fig. 10a). A caveat is that simulated egg distributions shifted north of 36° N during Regimes 2 and 3, which is outside the CalCOFI sampling area (30°–36° N).

Simulated larval consumption rate and zooplankton volume data collected in CalCOFI both showed a

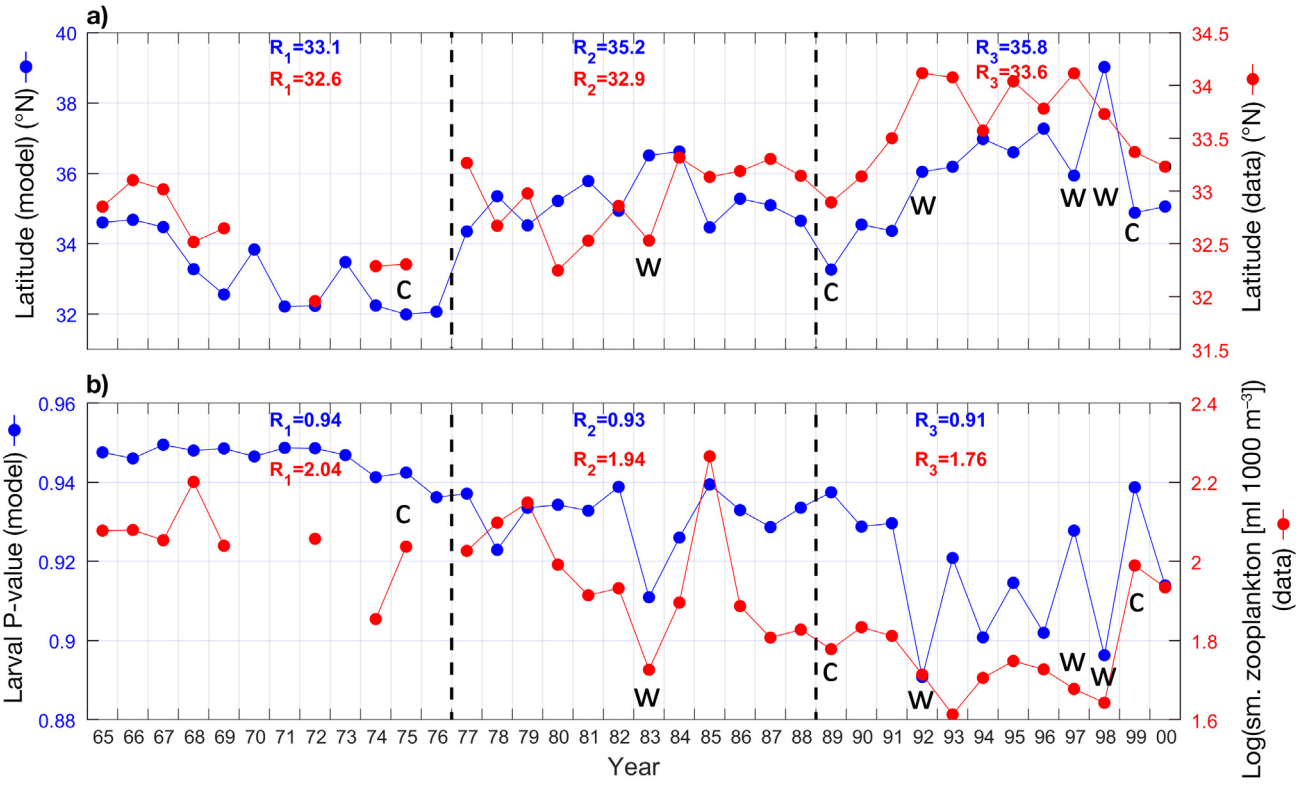

Fig. 10. (a) Mean latitude of modeled egg distributions (blue dots) against data (red dots) and (b) larval consumption rate expressed through P-value (blue dots) against log-scale small zooplankton volume data (ml 1000 m^{-3}) (red dots) their correlation coefficient was $r = -0.60$ (p = 0.0016). Egg distribution and zooplankton data were derived from California Cooperative Oceanic Fisheries Investigations survey program (CalCOFI; Bograd et al. 2003, Gallo et al. 2019). The averaged anomalies (R_1, R_2, and R_3) were calculated for simulated and observed values for each regime

clear downward trend over the 3 regimes (r = 0.66, p < 0.001, Fig. 10b). Furthermore, averaged juvenile and adult consumption rates were much less correlated to the zooplankton data (r = 0.18, p = 0.39 and r = 0.35, p = 0.01, respectively), suggesting that the correlation with larval consumption was meaningful. We also note that annual averaged model-domain zooplankton concentration was itself correlated with zooplankton data (r = 0.48, p = 0.015, data not shown).

3.9. Synthesis

Our analysis of extreme years and regimes within the historical simulation showed consistent responses of early life stages of anchovy to warm conditions and reduced food. Across all years, recruitment success (rec/eggs) was positively related to larval and egg survival, juvenile growth, and when spawning in cold years occurred more towards the south (Table 3).

The major drivers of lowered rec/eggs in warm years and in warmer regimes (2 and 3) were the reduced rates of growth and survival during egg, larval, and juvenile stages that were associated with exposure of the early life stages to warmer temperatures during anomalously warm years (Fig. 11). This exposure occurred as a consequence of the northward shift in spawning habitat and to some degree the northward movement of adults in response to warmer temperatures (and less so to changes in zooplankton) prior to spawning. More specifically, anomalies of rec/eggs were generally higher for the cold versus warm years (Fig. 11a) and progressed from positive to negative for the regimes (Fig. 11b). An exception was the cold year of 1999 that showed reduced rec/eggs despite the cooler conditions. Spawning shifted north in warm years and in Regimes 2 and 3. More reproduction occurred in the south in cold years and Regime 1, whereas southern reproduction switched to negative anomalies for warm years and Regimes 2 and 3 (Fig. 11). This switch is flipped when the proportion of spawning in the northern subregion is considered: cold years and regimes showed negative anomalies, and warm years and regimes showed red anomalies. While EYS survival was mixed among warm and cold years (Fig. 11a), a clear pattern of

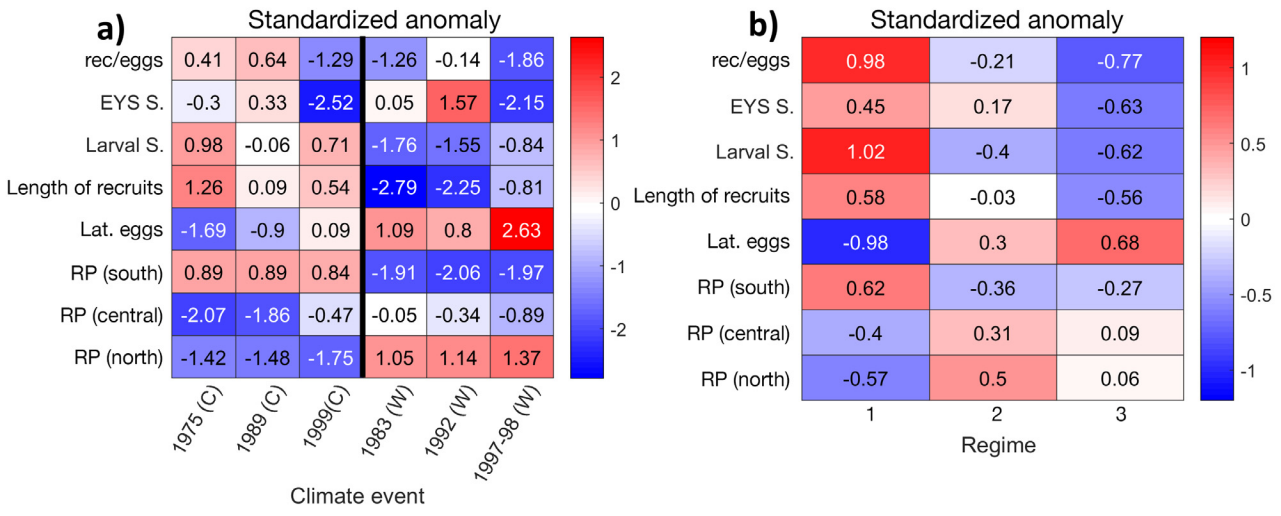

Fig. 11. Annual standardized anomalies of recruitment per total egg production (rec/eggs), egg and yolk-sac larva survival (EYS S.), larval survival (Larval S.), average length of recruits, mean latitude of egg distributions (Lat. eggs), and reproductive potential (RP) in the southern, central, and northern subregions for (a) the warm (W) and cold (C) extreme years and (b) the 3 regimes during 1965–2000

gradual progression from negative to positive anomalies (blue to red) was seen for the regimes (Fig. 11b). Anomaly changes in larval survival (determined by growth) and juvenile growth (length of recruits) were consistent among extreme years and regimes. Both had relatively positive anomalies for cold years and Regime 1 but had negative anomalies for warm years and Regimes 2 and 3 (Fig. 11).

4. DISCUSSION

Using models that cover many ecosystem components from primary producers to fish and top predators (the so-called end-to-end models) to attribute how climate-driven forcing can propagate throughout a marine ecosystem has received increasing attention (Travers et al. 2007, Rose et al. 2010). We focused here on the environmental controls of recruitment success in northern anchovy in extreme years (El Niño, La Niña) and different regimes using the 1965–2000 simulation. Our analysis of a model simulation showed the interaction of temperature with spawning movement leading to spatial shifts in warm years and regimes, eventually resulting in lowered recruitment success. The fact that modelled responses were generally, but not always, consistent within warm or cold years and among years within each regime demonstrates the challenges in cause-and-effect analysis of recruitment dynamics (Houde 2008). The model we used has the benefit of being developed based on the extensive study of northern anchovy in the California Current (Sydeman et al. 2020).

4.1. Anchovy response to climate variability

We used all years and comparison of cold versus warm years and cold versus warm regimes to follow the temperature and food signals from spatial shifts in spawning through eggs, larvae, and juveniles, and finally to recruitment. Warmer conditions caused lower recruitment success due to the synergistic effect of reduced egg and larval survival rates combined with adult spawning occurring farther north. This trend was seen when the 3 regimes were compared, although there was variation on a year-to-year basis, and not all extreme years showed the same patterns. For example, simulated anchovy showed a contrasting response (reduced recruitment and lowered EYS survival) during the cold year 1999. A possible explanation is that while 1999 was a cold year, it was influenced by the immediate year before, which was a warm year. All responses of extreme years and regimes showed various degrees of responses, even when following the general pattern, emphasizing the complexity of anchovy responses to inter-annual variation in environmental conditions.

Recruits tended to be distributed in the northern subregions of the CCS domain under warm conditions that corresponded with the northward shift in spawning habitat. However, the final distribution of juveniles was the result of circulation and survival

effects in egg and larval stages combined with the behavioral movement of juveniles in response to temperature and their zooplankton prey. Generally, larval distributions were found farther south compared to egg distributions (Fig. 12) mainly due to egg transport via circulation. Once they reached the juvenile stage, individuals tended to shift slightly to the north compared to larval distributions and also farther inshore (data not shown), as a result of behavioral movement of the juveniles responding to the local locations of optimal temperature and high zooplankton concentrations. Although direct observations are not available to confirm the north-to-south-to-north pattern from eggs to larvae to recruits in our simulation, these results agreed with the fish transport model of Weber et al. (2015), who showed that that eggs and larvae of another small pelagic fish (sardine) in the CCS were advected southward towards the US-Mexico border, and speculated that juveniles likely perform a northward movement to avoid oligotrophic waters and maximize recruitment.

Fish populations respond actively to environmental changes by shifting their locations to habitat that supports reproduction and survival of offspring (Perry et al. 2005, Rose 2005, Sundby & Nakken 2008, Ganias 2014). Our contrasts of extreme years and regimes showed shifts in the location of the optimal temperature window for spawning. The model did not explicitly include a spawning migration of anchovy, so the same movement algorithm used for hour-by-hour dynamics was responsible for their movement responses to broad-scale shifts in temperature. Simulated spawning of anchovy shifted north in response to warmer conditions but not enough to simply offset the warmer temperatures, and eggs in Regime 3 (the warmest regime) experienced cooler temperatures. Despite the general warming, averaged EYS survival anomaly decreased in Regime 2 compared to Regime 1 and declined further during the warmest Regime 3. Egg stage duration is temperature-dependent, and warmer temperatures should therefore result in higher survival, given that daily egg mortality rate is the same for all years. As the temperature anomalies associated with the sequential regimes increased, eggs occurred farther north but with a higher percent experiencing the lower bounds of the temperature window for reproduction (11.5–16.5°C). The majority of eggs were distributed south of 34° N in Regime 1, farther north (mainly between 33°–38° N) in Regime 2, and even farther north (34°–40° N) in Regime 3. Yet, counter-intuitively, the percent of eggs experiencing relatively cool temperatures (<13°C) increased across the regimes (26%, 35%, and 44% for R_1, R_2 and R_3, respectively). This demonstrates how temperature- and state-dependent reproductive success of the individual combines with behavioral movement, and then when superimposed on complicated spatial and temporal temperature and prey fields, can generate unexpected results (i.e. eggs experience cooler temperatures under warmer environmental conditions).

With regard to larval growth, warming of the CCS during El Niño and across the 3 regimes tended to decrease SZ and LZ concentrations available to larvae, leading to a decrease in their consumption rate. This induced a decrease in larval growth rate, and there-

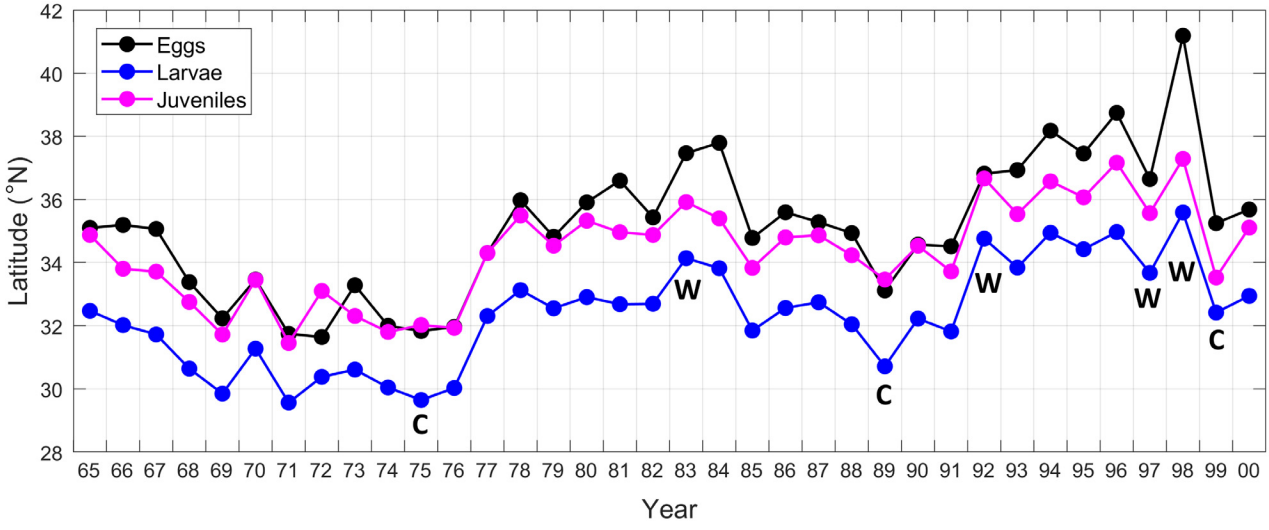

Fig. 12. Latitudinal centers of eggs (black dots), larvae (blue dots), and juvenile recruits (magenta dots) computed for each year of the historical simulation for 1965–2000. C and W: cold (La Niña) and warm (El Niño) extreme years within the historical simulation, respectively

fore an increase in the transition time from larval to juvenile stages (on average plus 2–10 d compared to the 1965–2000 average) and a longer exposure to stage-specific mortality. Thus, warm conditions resulted in a decline in larval survival. Conversely, the cooler periods during Regime 1 and the La Niña years of 1975 and 1999 were aligned with increased zooplankton concentrations, which generally favored larval survival. A notable exception occurred in 1989 (cold), though, when larval consumption rate was slightly above average, but larval survival was slightly below average. This model result is probably related to the match of a sufficient number (although still low) of larval model super-individuals with high worth (high contribution to the population) located in low prey conditions, influencing the average survival. It is worth noting that the transition between positive and negative anomalies in zooplankton for larvae was not associated with specific subregions during ENSO events but rather prevailed throughout the entire CCS domain. On the regime scale, however, negative zooplankton anomalies were more intense in the central CCS in Regime 2 and extended to the entire CCS domain in Regime 3. Overall, the EYS and larval survival findings conceptually agreed with other model studies that have confirmed the importance of a spatiotemporal match of early fish stages with a favorable environment to ensure good feeding conditions and high survival (Daewel et al. 2011, Kristiansen et al. 2011, Siddon et al. 2013).

4.2. Model evaluation

Our 3 direct comparisons of model results to empirically based estimates showed both significant deviations and reasonable agreements. Simulated recruitment and annual eggs (or SSB), when viewed in terms of numbers and biomass, showed a broad peak during the 1980s, while observed values showed a more rapid decline by 1975. Our analysis was based on the ratio (rec/eggs) rather than the values of recruitment and SSB, and anomalies of recruitment success from the model and empirical data also showed disagreement in the form of a downward trend in the model but not in the data. Averaging by regime resulted in better agreement, as averaged annual anomalies showed a decline in both the historical simulation and empirical data. We computed various versions of recruitment success using SSB and total eggs, and using recruitment data from Fissel et al. (2011), which were not adjusted to environmental conditions, all with similar results.

The remaining 2 model versus empirical data comparisons showed better agreement, providing greater support for our simulation. Averaged latitude centers of simulated egg distributions and predicted larval consumption versus field-based zooplankton densities showed good overall agreement. Spatial shifts in reproduction and larval growth are important drivers of our simulated responses in recruitment success. Our results allow for within-model analyses and interpretation at the level of bottom-up drivers of anchovy recruitment under warm versus cold conditions but are not valid as predictions for specific years.

There is qualitative evidence to corroborate some of the predicted results for certain ones of the extreme years in our simulation period. Model prediction of reduced larval survival and juvenile growth for the 1983 El Niño conditions was in general agreement with Fiedler et al. (1986), who reported that larval mortality was high in the spring of 1983 (implying low survival), and the average length of juveniles in the CalCOFI region decreased from around 83.5 mm during 1980–1982 to 71.9 mm in 1983. Anchovies responded favorably to the colder temperature conditions of 1985 combined with the increase in zooplankton predicted from the NEMURO model (Fig. 2b). Thus, in 1985, the center of spawning shifted to the south (34.4° N, Fig. 10a) compared to 1983 (36.5° N, Fig. 10a), larval survival anomaly was positive (+0.012%, Fig. 7c), juveniles achieved better growth (79.5 mm, Fig. 8), and simulated rec/eggs anomaly was higher than in 1983 (Fig. 4). This recovery agreed qualitatively with the observed recovery of juvenile growth described by Fiedler et al. (1986). They reported that juvenile length increased from 71.9 mm in 1983 to 79.4 mm in 1985, and there was a southward shift of eggs (the core of the egg distributions was found north of ~32.5° N in 1983 and south of ~32.5° N in 1985). Additionally, a return to more abundant copepod species in 1985 compared to the 1983 El Niño event was documented in field studies (Rebstock 2001). This was also in agreement with the transition of modeled zooplankton anomalies from a negative anomaly in 1983 (–0.059 mmolN m^{-3}) to a positive one in 1985 (+0.017 mmolN m^{-3}, Fig. 2b). However, the increase of simulated rec/eggs in 1985 did not agree with the empirically based rec/eggs that decreased slightly in 1985 compared to 1983 (Fissel et al. 2011). We note that in our analysis, we focused on year-specific rec/SSB and rec/eggs to estimate the response of anchovy to climate variation. Another approach would be to use lagged SSB (or eggs) as an indicator of recruitment. However, we did not use this approach since it would smooth recruit-

ment variability because multiple ages contribute to SSB each year.

Model simulation results of unfavorable conditions for anchovy after the warming in 1992 were also in general agreement with reported empirical data. The IBM predicted a notable decline in larval survival between 1992 and 1998 (Fig. 7d), which was related to negative zooplankton anomalies in Regime 3. This was consistent with the observed declining trend of larvae-to-eggs ratio (i.e. $\log_{10}$[larvae/eggs]) in southern California (MacCall et al. 2016) and the data analysis by Smith (1995), who reported an increase in temperature, a steep decrease in plankton biomass, and very low abundance of larvae from 1992 to 1994.

Finally, the model simulated a realistic response of anchovy to the relatively warmer period 1976–1977 within the generally cold Regime 1. Model-domain temperature anomalies shifted for the first time from negative in Regime 1 to positive in 1977–1978 (+0.4°C), and model-domain zooplankton anomalies shifted from positive in Regime 1 to negative in 1977–1978 (–0.017 mmolN m^{-3}). Modeled anchovy spawning habitats markedly shifted northward in 1977–1978 (Fig. 10a), and EYS survival increased sharply (Fig. 7b), whereas larval survival and juvenile growth declined drastically (Figs. 7d & 8). Additionally, modeled recruitment anomaly was low, being in accordance with estimated recruitment. Our findings generally matched the observed patterns of less zooplankton biomass and elevated sea surface temperature (McGowan et al. 2003), as well as high mortality of anchovy larvae due to starvation in the regime shift in 1977 (Lasker 1988).

4.3. Future opportunities

Our analysis of a long-term historical simulation indicated that cold periods generally tended to favor anchovy, whereas warm periods resulted in poor growth and survival of anchovy. This broadly aligns with the hypothesis of 'cool anchovy regime' in the CCS over the previous century (Chavez et al. 2003). However, the warm state observed in the CCS after 2014 (our simulation ended in 2000) was associated with increased anchovy egg and larval abundance in the CalCOFI area and high recruitment, especially during the El Niño of 2015–2016 (Thompson et al. 2019). Additionally, despite the cold conditions from 1999–2013, empirical data indicate that the anchovy population did not thrive (Sydeman et al. 2020). The current status of the anchovy population seems contradictory to historical knowledge and poses an excellent challenge for our model to be tested for the years 2014–2021, with the goal of identifying the underlying mechanisms that favored anchovy under recent, apparently warm conditions.

The cool-is-good paradigm for anchovy proposed by Chavez et al. (2003) was a qualitative description based on broad spatial and temporal scales using macro-level indicators, including coastal thermocline depths, nutrient supply, and productivity. Anchovy (and sardine) responses also have an important site-specific aspect, and there are within-ecosystem differences not well captured by macro-level indicators of ecosystem status. One hypothesis for model testing is that anchovy in the CCS inhabit relatively nearshore habitats that are influenced by coastal wind-driven upwelling and rivers (Checkley et al. 2017), and which can be missed by macro-level indicators. A possibility is that the coastal zone may remain productive and suitable for anchovy even when the large-scale conditions indicate overall warm conditions. Another possible hypothesis is that anchovy responses to El Niño perturbations (and other warm conditions) may occur under different time scales (e.g. instantaneous for spawning distribution, time-lagged for recruitment, and time-integrated for biomass, Ohman et al. 2017), which lead to complicated responses in recruitment from temporal and spatial match/mismatch of anchovy with its favorable environment (Kristiansen et al. 2011, Checkley et al. 2017, Politikos et al. 2018). The ecosystem response of the CCS to the recent warm conditions was complicated and likely previously undocumented (Thompson et al. 2019). This suggests that fluctuations in anchovy populations may be driven both by short- and long-term climate variation and from conditions that manifest spatially and temporally to create differential effects among habitats and life stages. Our existing model results showed that the relationship between regional climate and anchovy recruitment was much more nuanced than a simple response to warm versus cold year types, and the simulated population exhibited high inter-annual variability even within similar year types and regimes.

The time period of the historical simulation analyzed here (1965–2000) was maintained, because we have confidence in model results for this time period. Given the recent dynamics of anchovy in the CCS, extending our model simulation beyond 2000 would provide a platform for systematically testing hypotheses for why anchovy benefit from recent warm years. An initial key step in the modeling would be to confirm the ROMS and NEMURO NPZD outputs (transport, temperature, zooplankton), both revisit-

ing the historical time period and for the new years added to the simulation. Other key steps would include possible refinement of bioenergetics, mortality, and movement parameters of the anchovy IBM to ensure simulated responses match empirical data for both warm years in the early years versus recent warm years. The updated, and possibly recalibrated, end-to-end model could then be used to test our understanding, and possible alternative hypotheses, of anchovy responses to cold and warm years.

The analysis of the end-to-end model reported here adds to the collection of population and food web models for forage fish in the CCS (Lluch-Cota 2013, Kaplan et al. 2019). Such models offer opportunities for exploratory analyses of candidate, and sometimes competing, hypotheses about factors influencing the population dynamics of small pelagic fishes (Checkley et al. 2017, Sydeman et al. 2020). In addition, the results from these models may also inform management decisions via increased understanding of possible complex responses and as part of management strategy evaluations (Siple et al. 2021). The end-to-end model used here was designed (i.e. individual-based, spatially detailed in 3 dimensions) to examine how spatial and temporal variation in habitat conditions would affect long-term (decadal scale) population dynamics (see also Politikos et al. 2018, Nishikawa et al. 2019, Fiechter et al. 2021) and can complement the other models more tailored (e.g. Punt et al. 2016, multi-species, age-structured, simplified spatially) to management questions related to harvesting.

5. CONCLUSIONS

Anthropogenic warming continues to have serious effects on the ocean environment. Improving our knowledge of climate variability effects on historical changes in fish stocks is invaluable to better understand how these stocks will respond under future conditions (King et al. 2015, Pepin 2016). The integration of fish physiological and behavioral processes within multi-trophic ecosystem models can improve our ability to characterize the relationship between fish and their environment (Petitgas et al. 2013, Checkley et al. 2017) and predict the impact of global warming on fish species (Okunishi et al. 2012). Our analysis here leveraged an existing model and historical simulation to improve our understanding of how warm versus cold conditions may affect anchovy recruitment in the CCS. The effects of climate variability on small pelagic fish species in the CCS (e.g. anchovy, sardine) are well studied (King et al. 2011, McClatchie 2014). An exciting challenge is to determine how to combine the methods and results across models and the rich database for the CCS to further our understanding of how to inform predictive analyses of climate variability on anchovy and other forage fish species. Such detailed forensics on results (model and data) should lead to better models through refinement of their formulations and targeted data collection and analyses.

Acknowledgements. We express our appreciation to Dr. Benjamin Fissel for providing us access to spawning biomass, egg abundance, and recruitment data for anchovy and for our valuable discussion during the comparison of the model results with the empirical data. This study was partially supported by a grant from the National Oceanic and Atmospheric Administration (NOAA) NA17OAR4310269.

LITERATURE CITED

Alheit J, Roy C, Kifani S (2009) Decadal-scale variability in populations. In: Checkley DM Jr, Alheit J, Oozeki Y, Roy C (eds) Climate change and small pelagic fish. Cambridge University Press, Cambridge, p 285–383

Asch RG (2015) Climate change and decadal shifts in the phenology of larval fishes in the California Current ecosystem. Proc Natl Acad Sci USA 112:E4065–E4074

Boggs CH (1991) Bioenergetics and growth of northern anchovy *Engraulis mordax*. Fish Bull 89:555–566

Bograd SJ, Checkley DA Jr, Wooster WS (2003) CalCOFI: a half century of physical, chemical and biological research in the California Current System. Deep Sea Res II 50: 14–16

Brunel T, Boucher J (2007) Long-term trends in fish recruitment in the north-east Atlantic related to climate change. Fish Oceanogr 16:336–349

Butler JL (1989) Growth during the larval and juvenile stages of the northern anchovy, *Engraulis mordax*, in the California Current during 1980-84. Fish Bull 87:645–652

Butler JL, Smith PE, Lo NCH (1993) The effect of natural variability of life-history parameters on anchovy and sardine population growth. CalCOFI Rep 34:104–111

Canales TM, Lima M, Wiff R, Contreras-Reyes JE, Cifuentes U, Montero J (2020) Endogenous, climate, and fishing influences on the population dynamics of small pelagic fish in the southern Humboldt Current Ecosystem. Front Mar Sci 7:82

Carton JA, Chepurin G, Cao X (2000) A Simple Ocean Data Assimilation analysis of the global upper ocean 1950–1995. Part 2: results. J Phys Oceanogr 30:311–326

Chavez F (1996) Forcing and biological impact of onset of the 1992 El Niño in central California. Geophys Res Lett 23:265–268

Chavez FP, Ryan J, Lluch-Cota SE, Nīquen M (2003) From anchovies to sardines and back: multidecadal change in the Pacific Ocean. Science 299:217–221

Checkley DM Jr, Barth J (2009) Patterns and processes in the California Current system. Prog Oceanogr 83:49–64

Checkley DM Jr, Alheit J, Oozeki Y, Roy C (eds) (2009) Climate change and small pelagic fish. Cambridge University Press, Cambridge

Checkley DM Jr, Asch RG, Rykaczewski RR (2017) Climate, anchovy, and sardine. Annu Rev Mar Sci 9:469–493

Clark WG, Hare SR, Parma AM, Sullivan PJ, Trumble RJ (1999) Decadal changes in growth and recruitment of Pacific halibut (*Hippoglossus stenolepis*). Can J Fish Aquat Sci 56:173–183

Daewel U, Peck MA, Schrum C (2011) Life history strategy and impacts of environmental variability on early life stages of two marine fishes in the North Sea: an individual-based modelling approach. Can J Fish Aquat Sci 68: 426–443

DeAngelis DL, Diaz SG (2019) Decision-making in agent-based modeling: a current review and future prospectus. Front Ecol Evol 6:237

DeAngelis DL, Grimm V (2014) Individual-based models in ecology after four decades. F1000Prime Rep 6:39

Deslauriers D, Chipps SR, Breck JE, Rice JA, Madenjian CP (2017) Fish bioenergetics 4.0: an R-based modeling application. Fisheries 42:586–596

Doney SC, Ruckelshaus M, Duffy JE, Barry JP and others (2012) Climate change impacts on marine ecosystems. Annu Rev Mar Sci 4:11–37

Drinkwater KF (2005) The response of Atlantic cod (*Gadus morhua*) to future climate change. ICES J Mar Sci 62: 1327–1337

Fiechter J, Rose KA, Curchitser EN, Hedstrom KS (2015) The role of environmental controls in determining sardine and anchovy population cycles in the California Current: analysis of an end-to-end model. Prog Oceanogr 138: 381–398

Fiechter J, Pozo Buil M, Jacox MG, Alexander MA, Rose KA (2021) Projected shifts in 21st century sardine distribution and catch in the California Current. Front Mar Sci 8:685241

Fiedler PC, Methot RD, Hewitt RP (1986) Effects of California El Niño 1982–1984 on the northern anchovy. J Mar Res 44:317–338

Fissel BE, Lo NCH, Herrick SF Jr (2011) Daily egg production, spawning biomass and recruitment for the central subpopulation of northern anchovy 1981–2009. CalCOFI Rep 52:116–135

Gallo ND, Drenkard E, Thompson AR, Weber ED and others (2019) Bridging from monitoring to solutions-based thinking: lessons from CalCOFI for understanding and adapting to marine climate change impacts. Front Mar Sci 6:695

Ganias K (ed) (2014) Biology and ecology of sardines and anchovies. CRC Press, Boca Raton, FL

Hare SR, Mantua NJ (2000) Empirical evidence for North Pacific regime shifts in 1977 and 1989. Prog Oceanogr 47: 103–145

Hayward TL (1993) Preliminary observations of the IYY-1991 El Nina in the California Current. CalCOFI Rep 34:21–29

Hofmann EE, Powell TM (1998) Environmental variability effects on marine fisheries: four case histories. Ecol Appl 8(Supplement):S23–S32

Houde ED (2008) Emerging from Hjort's shadow. J Northwest Atl Fish Sci 41:53–70

Humston R, Olson DB, Ault JS (2004) Behavioral assumptions in models of fish movement and their influence on population dynamics. Trans Am Fish Soc 133:1304–1328

Hunter JR (1976) Culture and growth of northern anchovy, *Engraulis mordax*, larvae. Fish Bull 74:81–88

Hunter JR (1981) Feeding ecology and predation of marine fish larvae. In: Lasker R (ed) Marine fish larvae: morphology, ecology, and relation to fisheries. University of Washington Press, Seattle, WA, p 33–77

Hunter JR, Macewicz BJ (1980) Sexual maturity, batch fecundity, spawning frequency, and temporal pattern of spawning for the northern anchovy, *Engraulis mordax*, during the 1979 spawning season. CalCOFI Rep 21: 139–149

Hunter JR, Macewicz BJ (1985a) Measurement of spawning frequency in multiple spawning fishes. In: Lasker R (ed) An egg production method for estimating spawning biomass of pelagic fish: application to the northern anchovy, *Engraulis mordax*. NOAA Technical Report NMFS 36. National Oceanographic and Atmospheric Administration, Springfield, VA, p 79–94

Hunter JR, Macewicz BJ (1985b) Rates of atresia in the ovary of captive and wild northern anchovy, *Engraulis mordax*. Fish Bull 83:119–136

Jacobson LD, Lo NCH, Herrick SF Jr, Bishop T (1995) Spawning stock biomass of the northern anchovy in 1995 and status of the coastal pelagic fishery during 1994. Administrative Report LJ-95-11. NMFS, SWFSC Admin, La Jolla, CA

Jung S, Pang IC, Lee JH, Choi I, Cha H (2014) Latitudinal shifts in the distribution of exploited fishes in Korean waters during the last 30 years: a consequence of climate change. Rev Fish Biol Fish 24:443–462

Kaplan IC, Francis TB, Punt AE, Koehn LE and others (2019) A multi-model approach to understanding the role of Pacific sardine in the California Current food web. Mar Ecol Prog Ser 617–618:307–321

King JR (ed) (2005) Report of the study group on the fisheries and ecosystem responses to recent regime shifts. PICES Scientific Report Number 28. North Pacific Marine Science Organization (PICES), Institute of Ocean Sciences, Sidney, BC

King JR, Agostini VN, Harvey CJ, McFarlane GA and others (2011) Climate forcing and the California Current ecosystem. ICES J Mar Sci 68:1199–1216

King JR, McFarlane GA, Punt AE (2015) Shifts in fisheries management: adapting to regime shifts. Philos Trans R Soc Lond B Biol Sci 370:20130277

Kishi MJ, Kashiwai M, Ware DM, Megrey BA and others (2007) NEMURO — a lower trophic level model for the North Pacific marine ecosystem. Ecol Modell 202:12–25

Kristiansen T, Drinkwater KF, Lough RG, Sundby S (2011) Recruitment variability in North Atlantic cod and match-mismatch dynamics. PLOS ONE 6:e17456

Large WG, Yeager SG (2009) The global climatology of an interannually varying air-sea flux data set. Clim Dyn 33: 341–363

Lasker R (1981) Factors contributing to variable recruitment of the northern anchovy *Engraulis mordax* in the California Current USA contrasting years 1975-1978. Rapp P-V Réun Cons Int Explor Mer 178:375–388

Lasker R (1988) Studies on the northern anchovy; biology, recruitment and fishery oceanography. In: Studies on fisheries oceanography, Proc 25th Anniversary Symp 'Fisheries and fishery oceanography in the coming century', Tokyo, 10–13 Nov 1986, Japanese Society of Fishery Oceanography, p 24–41

Lluch-Belda D, Lluch-Cota DB, Hernandez-Vazquez S, Salinas-Zavala C, Schwartzlose RA (1991) Sardine and anchovy spawning as related to temperature and upwelling in the California Current system. CalCOFI Rep 32:105–111

Lluch-Cota SE (2013) Modeling sardine and anchovy low-frequency variability. Proc Natl Acad Sci USA 110: 13240–13241

Lo NCH, Smith PE, Butler JL (1995) Population growth of northern anchovy and Pacific sardine using stage-specific matrix models. Mar Ecol Prog Ser 127:15–26

Lo NCH, Macewicz BJ, Griffith DA (2005) Spawning biomass of Pacific sardine (*Sardinops sagax*), from 1994–2004 off California. CalCOFI Rep 46:93–112

Lo NCH, Macewicz BJ, Griffith DA (2011) Migration of Pacific sardine (*Sardinops sagax*) off the west coast of United States in 2003–2005. Bull Mar Sci 87:395–412

Lynn RJ, Bograd SJ (2002) Dynamic evolution of the 1997–1999 El-Niño–La-Niña cycle in the southern California Current System. Prog Oceanogr 54:59–75

Lynn RJ, Schwing FB, Hayward TL (1995) The effect of the 1991–1993 ENSO on the California Current System. CalCOFI Rep 36:57–71

MacCall A (2011) The sardine-anchovy puzzle. In: Jackson J, Alexander K, Sala E (eds) Shifting baselines: the past and the future of ocean fisheries. Island Press, Washington, DC, p 47–58

MacCall AD, Batchelder H, King J, Mackas D and others (2005) Recent ecosystem changes in the California Current system. In: King JR (ed) Report of the study group on the fisheries and ecosystem responses to recent regime shifts. North Pacific Marine Science Organization (PICES), PICES Scientific Report 28, Sidney, BC, p 65–86

MacCall AD, Sydeman WJ, Davison PC, Thayer JA (2016) Recent collapse of northern anchovy biomass off California. Fish Res 175:87–94

Mantua N (2004) Methods for detecting regime shifts in large marine ecosystems: a review with approaches applied to North Pacific data. Prog Oceanogr 60:165–182

McClatchie S (2014) Regional fisheries oceanography of the California Current System. Springer, Dordrecht

McGowan JA, Bograd SJ, Lynn RJ, Miller AJ (2003) The biological response to the 1977 regime shift in the California Current. Deep Sea Res II 50:2567–2582

Murphree T, Reynolds C (1995) El Ninõ and La Ninã effects on the northeast Pacific: the 1991-1993 and 1988-1989 events. CalCOFI Rep 36:45–56

Nakayama SI, Takasuka A, Ichinokawa M, Okamura H (2018) Climate change and interspecific interactions drive species alternations between anchovy and sardine in the western North Pacific: detection of causality by convergent cross mapping. Fish Oceanogr 27:312–322

Nishikawa H, Curchitser EN, Fiechter J, Rose KA, Hedstrom K (2019) Using a climate-to-fishery model to simulate the influence of the 1976-1977 regime shift on anchovy and sardine in the California Current System. Prog Earth Planet Sci 6:9

Ohman MD, Mantua N, Keister J, Garcia-Reyes M, McClatchie S (2017) ENSO impacts on ecosystem indicators in the California Current System. CLIVAR & OCB Newsletter 15:8–15

Okunishi T, Ito S, Hashioka T, Sakamoto TT and others (2012) Impacts of climate change on growth, migration and recruitment success of Japanese sardine (*Sardinops melanostictus*) in the western North Pacific. Clim Change 115:485–503

Okunishi T, Yamanaka Y, Ito S (2009) A simulation model for Japanese sardine (*Sardinops melanostictus*) migrations in the western North Pacific. Ecol Modell 220:462–479

Overholtz WJ, Hare JA, Keith CM (2011) Impacts of interannual environmental forcing and climate change on the distribution of Atlantic mackerel on the U.S. Northeast Continental Shelf. Mar Coast Fish 3:219–232

Overland J, Rodionov S, Minobe S, Bond N (2008) North Pacific regime shifts: Definitions, issues and recent transitions. Prog Oceanogr 77:92–102

Palacios DM, Bograd SJ, Mendelssohn R, Schwing FB (2004) Long-term and seasonal trends in stratification in the California Current, 1950–1993. J Geophys Res Oceans 109:C10016

Pecquerie L, Petitgas P, Kooijman SALM (2009) Modeling fish growth and reproduction in the context of the Dynamic Energy Budget theory to predict environmental impact on anchovy spawning duration. J Sea Res 62:93–105

Pepin P (2016) Reconsidering the impossible - linking environmental drivers to growth, mortality and recruitment of fish. Can J Fish Aquat Sci 73:205–215

Perry AL, Low PJ, Ellis JR, Reynolds JD (2005) Climate change and distribution shifts in marine fishes. Science 308:1912–1915

Petitgas P, Rijnsdorp AD, Dickey-Collas M, Engelhard GH and others (2013) Impacts of climate change on the complex life cycles of fish. Fish Oceanogr 22:121–139

Petrik CM, Duffy-Anderson JT, Mueter F, Hedstrom K, Curchitser EN (2015) Biophysical transport model suggests climate variability determines distribution of walleye pollock early life stages in the eastern Bering Sea through effects on spawning. Prog Oceanogr 138: 459–474

Politikos DV, Curchitser EN, Rose KA, Checkley DM Jr, Fiechter J (2018) Climate variability and sardine recruitment in the California Current: a mechanistic analysis of an ecosystem model. Fish Oceanogr 27:602–622

Punt AE, MacCall AD, Essington TE, Francis TB and others (2016) Exploring the implications of the harvest control rule for Pacific sardine, accounting for predator dynamics: a MICE model. Ecol Modell 337:79–95

Rebstock GA (2001) Long-term stability of species composition in calanoid copepods off southern California. Mar Ecol Prog Ser 215:213–224

Rose GA (2005) On distributional responses of North Atlantic fish to climate change. ICES J Mar Sci 62:1360–1374

Rose KA, Allen JI, Artioli Y, Barange M and others (2010) End-to-end models for the analysis of marine ecosystems: challenges, issues, and next steps. Mar Coast Fish 2:115–130

Rose KA, Fiechter J, Curchitser EN, Hedstrom K and others (2015) Demonstration of a fully-coupled end-to-end model for small pelagic fish using sardine and anchovy in the California Current. Prog Oceanogr 138:348–380

Salvatteci R, Field D, Gutiérrez D, Baumgartner T and others (2018) Multifarious anchovy and sardine regimes in the Humboldt Current System during the last 150 years. Glob Change Biol 24:1055–1068

Scheffer M, Baveco JM, DeAngelis DL, Rose KA, van Nes EH (1995) Super-individuals a simple solution for modelling large populations on an individual basis. Ecol Modell 80:161–170

Scura ED, Jerde CW (1977) Various species of phytoplankton as food for larval northern anchovy, *Engraulis mordax*, and relative nutritional value of the dinoflagellates *Gymnodinium splendens* and *Gonyaulax polyedra.* Fish Bull 75:577–583

Shchepetkin AF, McWilliams JC (2005) The regional oceanic modeling system (ROMS): a split-explicit, free-surface,

topography-following-coordinate oceanic model. Ocean Model 9:347–404

Shoji J, Toshito S, Mizuno K, Kamimura Y, Hori M, Hirakawa K (2011) Possible effects of global warming on fish recruitment: shifts in spawning season and latitudinal distribution can alter growth of fish early life stages through changes in daylength. ICES J Mar Sci 68: 1165–1169

Siddon EC, Kristiansen T, Mueter FJ, Holsman KK and others (2013) Spatial match-mismatch between juvenile fish and prey provides a mechanism for recruitment variability across contrasting climate conditions in the eastern Bering sea. PLOS ONE 8:e84526

Simpson JJ (1983) Large-scale thermal anomalies in the California Current during the 1982-1983 El Niño. Geophys Res Lett 10:937–940

Siple, MC, Essington TE, Barnett LAK, Scheuerell MD (2020) Limited evidence for sardine and anchovy asynchrony: re-examining an old story. Proc R Soc B 287: 20192781

Siple MC, Koehn LE, Johnson KF, Punt AE and others (2021) Considerations for management strategy evaluation for small pelagic fishes. Fish Fish 22:1167–1186

Smith PE (1995) A warm decade in the Southern California bight. CalCOFI Rep 36:120–126

Sundby S, Nakken O (2008) Spatial shifts in spawning habitats of Arcto-Norwegian cod related to multidecadal climate oscillations and climate change. ICES J Mar Sci 65: 953–962

Sydeman WJ, Dedman S, García-Reyes M, Thompson SA, Thayer JA, Bakun A, MacCall D (2020) Sixty-five years of northern anchovy population studies in the southern California Current: a review and suggestion for sensible management. ICES J Mar Sci 77:486–499

Takahashi M, Watanabe Y, Yatsu A, Nishida H (2009) Contrasting responses in larval and juvenile growth to a climate-ocean regime shift between anchovy and sardine. Can J Fish Aquat Sci 66:972–982

Thayer JA, MacCall AD, Sydeman WJ, Davison PC (2017) California anchovy population remains low, 2012–2016. CalCOFI Rep 58:1–8

Thompson AR, Schroeder ID, Bograd SJ, Hazen EL and others (2019) State of the California Current 2018-19: a novel anchovy regime and a new marine heatwave? CalCOFI Rep 60:1–65

Travers M, Shin YJ, Jennings S, Cury P (2007) Towards end-to-end models for investigating the effects of climate and fishing in marine ecosystems. Prog Oceanogr 75:751–770

Urtizberea A, Fiksen O, Folkvord A, Irigoien X (2008) Modelling growth of larval anchovies including diel feeding patterns, temperature and body size. J Plankton Res 30: 1369–1383

Walsh HJ, Richardson DE, Marancik KE, Hare JA (2015) Long-term changes in the distributions of larval and adult fish in the Northeast U.S. Shelf Ecosystem. PLOS ONE 10:e0137382

Wang SB (1998) Comparative studies of the life history and production potential of bay anchovy *Anchoa mitchilli* and northern anchovy *Engraulis mordax*: an individual-based modeling approach. PhD thesis, University of South Alabama, Mobile, AL

Watkins KS, Rose KA (2013) Evaluating the performance of individual-based animal movement models in novel environments. Ecol Modell 250:214–234

Weber ED, Chao Y, Chai F, McClatchie S (2015) Transport patterns of Pacific sardine *Sardinops sagax* eggs and larvae in the California Current System. Deep Sea Res I 100:127–139

Werner FE, Perry RI, Lough RG, Naimie CE (1996) Trophodynamic and advective influences on Georges Bank larval cod and haddock. Deep Sea Res II 43:1793–1822

Xu Y, Chai F, Rose KA, Niquen MC, Chavez FP (2013) Environmental influences on the interannual variation and spatial distribution of Peruvian anchovy (*Engraulis ringens*) population dynamics from 1991 to 2007: a three-dimensional modelling study. Ecol Modell 264:64–82

Zweifel JR, Lasker R (1976) Prehatch and posthatch growth of fishes — a general model. Fish Bull 74:609–621

Editorial responsibility: Corinna Schrum (Guest Editor), Geesthacht, Germany
Reviewed by: D. Benkort and 2 anonymous referees

Submitted: January 25, 2021
Accepted: August 2, 2021
Proofs received from author(s): November 16, 2021